Faculteit Industriële Ingenieurswetenschappen
master in de industriële wetenschappen: chemie

Masterthesis

Optimization of the green synthesis of potential anti-ageing compounds

PROMOTOR :
Prof. dr. ir. Leen THOMASSEN

PROMOTOR :
Prof. dr. Alina GHINET

BEGELEIDER :
PhD. Lisa BONIN

Othmane Birbouz
Scriptie ingediend tot het behalen van de graad van master in de industriële wetenschappen: chemie

▶▶ UHASSELT   KU LEUVEN

2021•2022
Faculteit Industriële Ingenieurswetenschappen
master in de industriële wetenschappen: chemie

Masterthesis

Optimization of the green synthesis of potential anti-ageing compounds

PROMOTOR :

Prof. dr. ir. Leen THOMASSEN

PROMOTOR :

Prof. dr. Alina GHINET

BEGELEIDER :

PhD. Lisa BONIN

Othmane Birbouz

Scriptie ingediend tot het behalen van de graad van master in de industriële wetenschappen: chemie

▶▶ UHASSELT   KU LEUVEN

PREFACE

This master's thesis was the most instructive and fascinating experience in my career as an engineering student. I would like to thank the research group Chimie Durable et Santé from the university of JUNIA HEI for giving me this big opportunity. I would also like to thank several people for their guidance, feedbacks and valuable advices.

First, I would like to express my sincere gratitude to prof. dr. Alina Ghinet for giving me this opportunity, but also for the countless help, advices and feedbacks I got during my research. I could always approach her if I had any questions or difficulties, and she always responded very friendly.

I would also like to sincerely thank prof dr. ir. Leen Thomassen for her numerous feedbacks and advices during the writing of this thesis.

I also want to thank Mr. Christophe Andre for his help, feedback and guidance on processing the data.

Another person I would like to thank is PhD student Lisa Bonin for her guidance and help during the experimental work. I could always rely on her when I had questions or difficulties.

My gratitude also goes to technician Adrian Sorin Nica for informing me about the use of the equipment in the lab and making sure everything goes as safe as possible. I also thank the other researchers in the lab for making it a very pleasant working space.

Finally, I would also like to thank my family and friends for their support. Special thanks goes to my parents for their support and confidence in me, but also my sister and role model, who has inspired me to challenge myself in order to achieve my goals.

Thank you all.

TABLE OF CONTENTS

LIST OF TABLES

LIST OF FIGURES

ABSTRACT

The research group Chimie Durable et santé from the university of JUNIA HEI is specialized in the chemistry of L-pyroglutamic acid (PGA) also known as the "forgotten amino acid", with a significant interest in sustainable chemistry. The research group has found compounds derived from PGA which have potential anti-ageing properties. The synthesis of target compounds needs two reaction steps which are: 1) *N*-carboxy benzylation and 2) an ester amidation. However, the optimal reaction conditions for the synthesis of this molecule are not fully known.

This thesis investigates sustainable reagents, solvents and ecocatalysts processed from metal contaminated plants. Reaction conditions such as the temperature and concentration are compared with each other by monitoring the reaction progress by ^{1}H-NMR.

The ecocatalysts showed promising results on the reaction rate. The other metal chlorides had better effect on the activation of the ester amidation reaction compared to $ZrCl_4$. Additionally, the +M electro donating effect on the amine for the ester amidation reaction had a positive effect on the reaction rate. The best results were obtained with 2,4-dimethoxybenzylamine as a reagent. The isolated yield for the *N*-carboxy benzylation and the ester amidation with the best reaction conditions, identified upon optimization study, were 73.4 % and 64.3 %, respectively. Ultimately, this study could be of interest for the industrializing of these type of reactions by the pharmaceutic or cosmetic industry.

ABSTRACT IN HET NEDERLANDS

De onderzoeksgroep Chimie Durable et Santé van de universiteit JUNIA Hei is gespecialiseerd in de chemie van L-pyroglutaminezuur (PGA), ook wel bekend als het 'vergeten aminozuur', met een behoorlijke interesse in duurzame chemie. De onderzoeksgroep heeft moleculen gevonden afgeleid van PGA met potentiële anti-veroudering eigenschappen. De synthese van doelverbindingen vergt twee reactiestappen, namelijk: 1) Een *N*-carboxy benzylatie, gevolgd door 2)een ester amidatie. De optimale reactieomstandigheden voor de synthese van deze moleculen zijn echter niet volledig gekend.

Deze studie onderzoekt duurzame reagentia, solventen en ecokatalysatoren afkomstig van metaal gecontamineerde planten. Reactieomstandigheden, zoals verschillende temperaturen, werden met elkaar vergeleken door de reactie op te volgen met ^{1}H-NMR.

De ecokatalysatoren toonden veelbelovende resultaten op de reactiesnelheid. De andere metaalchloriden hadden een beter effect op de activering van de ester amidatie reactie dan $ZrCl_4$. Bovendien had een toenemend elektron duwend effect op de amine voor de esteramidatie reactie een positief effect op de reactiesnelheid. De beste resultaten werden verkregen met 2,4-dimethoxybenzylamine als reagens. De opbrengst voor de *N*-carboxy benzylatie en de ester amidatie met de beste reactieomstandigheden, vastgesteld door de optimalisatiestudie, gaven een rendement van respectievelijk 73.4 % en 64.3 %. Uiteindelijk zou deze studie van belang kunnen zijn voor de industrialisering van dit soort reacties door de chemische industrie.

1. INTRODUCTION

1.1. Context

The awareness of global challenges such as climate change, biodiversity loss, pollution and waste is increasing. This causes governments to take actions to tackle these problems. The traditional linear economy has shown that Earth's valuable resources are starting to diminish. Now, the linear economy must be redesigned into a circular economy where: waste and pollution are eliminated, products and materials are recirculated and nature is restoring some balances which are now unbalanced [1]. Since the chemical industry plays a big role in this transition, there is more need for green chemistry. Specifically, there is more need for eco-friendly solvents, reagents, catalysts, waste management etc. Green chemistry implies the use of sustainable and safe chemical activities. This includes, sustainability for human health and environment [2].

The solvents, reagents and catalysts that originate from renewable sources such as agricultural crops or from various waste streams can be considered as eco-friendly. An example is the use of CO_2 from internal combustion engine exhausts as a reagent to tackle global warming by valorising this molecule. Global warming can be directly correlated with the industrial activities of humanity, which cause a disturbance in the carbon cycle. The main problem is burning fossil fuels as an energy source, which adds the majority of CO_2 in the atmosphere and thus, causes an increase in temperature because of its heat absorbing properties [3]. Due to the rising CO_2 concentration in the atmosphere, there is a need for more carbon capture use (CCU) instead of only carbon capture storage (CCS) technology. The CCS Technique does not fit in the circular economy because it only removes the emitted CO_2 from the atmosphere or prevents it from being emitted in the atmosphere. The captured CO_2 is then stored underground or in storages [4].

In the CCS technique the CO_2 is seen as waste, whereas for CCU it is seen as a resource. The transformation of CO_2 into different useful molecules could make the carbon capture techniques more affordable. Currently, the transformation of CO_2 to urea is the largest industrialized CO_2 transformation technique. 200 Mt of urea is produced per year and 140 Mt of CO_2 per year is utilized for this. This is one pathway of utilizing CO_2. The other pathways are by using CO_2 as: CO_2-based fuels; microalgae fuels and products; concrete building materials; enhanced oil recovery; bio-energy with CCS (BECCS); enhanced weathering; forestry techniques such as afforestation/reforestation, forest management and wood products; land management via soil carbon sequestration techniques; and biochar. Table 1 shows the range estimates of the potential for CO_2 utilization and present-day breakeven cost [5].

Table 1: Range estimates for CO₂ utilization and present-day breakeven cost, reproduced from [5, p. 92]

pathway	Removal potential in 2050 (Mt CO_2 removed per year)	Utilization potential in 2050 (Mt CO_2 utilized per year)	Breakeven cost of CO_2 utilization (2015 US$ per tonne CO_2 utilized
Conventional utilization			
Chemicals	Around 10 to 30	300 to 600	-$80 to $320
Fuels	0	1000 to 4200	$0 to $670
Microalgae	0	200 to 900	$230 to $920
Concrete building materials	100 to 1400	100 to 1400	-$30 to $70
Enhanced oil recovery	100 to 1800	100 to 1800	-$60 to -$45
Non-conventional utilization			
BECCS	500 to 5000	500 to 5000	$60 to $160
Enhanced weathering	2000 to 4000	Not determined	Less than $200
Forestry techniques	500 to 3600	70 to 1100	-$40 to $10
Land management	2300 to 5300	900 to 1900	-$90 to -$20
Biochar	300 to 2000	170 to 1000	-$70 to -$60

This thesis is commissioned by the research group Chimie Durable et Santé of the university JUNIA HEI in Lille. The research group is engaged in organic chemistry with a significant interest in sustainable chemistry for the development towards a circular economy. The laboratory's research is devoted to the synthesis of new molecules that are important for human and plant health. Furthermore, the research group has a recognised expertise in the chemistry of PGA, which originates from sugar beet molasses. This molecule is used as a basic synthon in several projects including this master's thesis topic [6].

One of the subjects of the research group is also the valorisation of CO_2. The plan is to synthesize useful molecules from CO_2 as a reagent. The objective is to make as many useful molecules from CO_2 as possible to be able to make a dent in the global carbon emissions. This project takes place in cooperation with the River project, which is funded by the Interreg North-West Europe program. The goal of the River project is to reduce or eliminate the pollutants emitted from inland waterway vessels. To eliminate the NO_X production from diesel engines, River wants to apply oxy-fuel technology and the emitted CO_2 will then be stored or used. Oxy-fuel technology is when diesel is burned with pure oxygen or pure oxygen mixed with recirculated flue gasses to control the temperature [7]. This highly concentrated CO_2 gas after combustion allows the storage of CO_2 or its use as a reagent in other reactions.

The main output of the River project is thus: CCS technology, carbon transformation or CCU and to create a roadmap for the utilisation of new engine technology with zero carbon emissions for inland waterway transportation. The project was created because of the rules adopted by the EU that aims to limit carbon emissions (Directive 97/68/EC,01/2017) [8]. This thesis will focus more on the subject of CCU to synthesize useful molecules. The useful molecules which will be further discussed are

potential anti-ageing compounds. These compounds could be interesting for the pharmaceutical or cosmetic industry to tackle ageing and possibly illnesses that come with ageing.

1.2. Anti-ageing properties

The synthesized anti-ageing compounds in this thesis will be tested on their potential anti-ageing properties. The principle of this anti-ageing concept is based on the inhibition of the RAGE receptor protein. This is a receptor for advanced glycation endproducts (RAGE) which is responsible for the accumulation of advanced glycation endproducts (AGEs). The AGEs are responsible for a cascade of intracellular signalling which produces: reactive oxygen species (ROS), immunoinflammatory effects, cellular proliferation or apoptosis. RAGE thus plays a role in pathological conditions such as cancer, diabetes, etc. because glycation is responsible for: loss of enzymatic function, protein cross-linking or aggregation [9].

By inhibiting this protein, the aging process could be slowed down due to the management of the immunoinflammatory pathologies. RAGE can bind to a diverse group of molecules from relatively low molecular weight to larger structures. An example of molecules it can bind to is *N*-carboxy-methyl-lysine which interacts with positively charged (Lys52, Lys110 and Arg98) and hydrophobic residues of RAGE V domain. Lys52, Lys110 and Arg98 are involved in binding the AGEs to RAGE [9]. The molecules synthesized in this study will be tested in another study on how they bind on RAGE and their effectivity.

1.3. Synthesis of the potential anti-ageing molecules

The synthesis of the potential anti-ageing molecule will be done with: sustainable reagents, solvents and catalysts. One of the sustainable reagents is CO_2. Generally, CO_2 can be used in chemical, photochemical and electrochemical reactions as C1 building block. This is a renewable way to add 1 carbon in a molecule and avoids the use of more toxic molecules such as CO, phosgene and oxalyl chloride. CO_2 fixation techniques in various solvents have made it possible to transform CO_2 into useful molecules such as urea, methanol, cyclic carbonates, carbamates and so on [10]. This thesis will go further on the *N*-carboxy benzylation of methyl L-pyroglutamate (PGM) followed by an ester amidation to synthesize the potential anti-ageing compounds. The synthesis of one target anti-ageing molecule is illustrated in Figure 1.
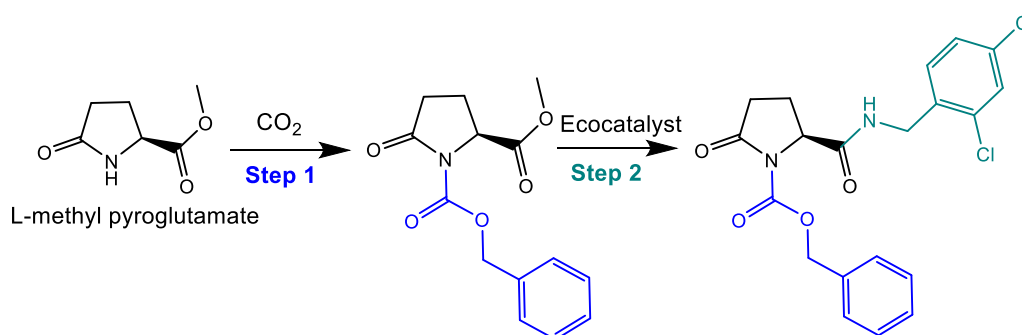
Figure 1: Reaction steps for the synthesis of the anti-ageing compound

15

In the research of Homerin et al., for the first step of the synthesis, CO_2 reacts with (PGM) and benzyl bromide together with Cs_2CO_3 as a base, tetrabutylammonium bromide (TBAB) as phase transfer agent and acetonitrile (ACN) or dimethyl formamide (DMF) as solvent [4]. This reaction is shown in figure 2.
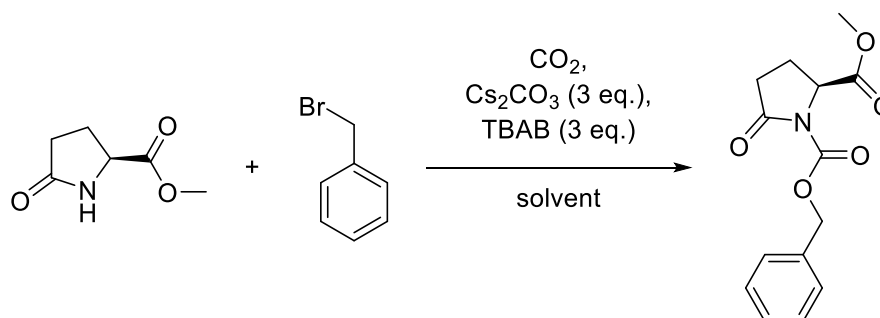
Figure 2: Step 1) N-carboxy benzylation of PGM with CO₂ and benzyl bromide [4, p. 2]

The purpose of the base Cs_2CO_3, for the reaction illustrated in figure 2, is to activate the nitrogen so that it attacks on the carbon of CO_2. Other bases were also studied by Homerin et al. such as: Rb_2CO_3, K_2CO_3, Na_2CO_3, K_3PO_4, KOH, t-BuOK, Et_3N and CsF. The base that gave the best yield was the Cs_2CO_3. The reason is because Cs_2CO_3 is a mild base which is not strong enough to result in a saponification reaction on the ester [4].

The function of the phase transfer agent TBAB, shown in figure 2, is to transport the reactive ions to the phase where they can react better with the other reagent [11]. In this reaction there is a liquid and a solid phase. The solid phase in this reaction is the base Cs_2CO_3. The PGM becomes activated on the solid phase and with the help of TBAB, the intermediate can be transported to the liquid phase where it then reacts with benzyl bromide. Homerin et al. studied a variety of phase transfer agents on the step 1 reaction. The phase transfer agents that allowed full conversion were TBAB, TBAI and TMAI [4].

The mechanism of this reaction is shown by figure 3 below.
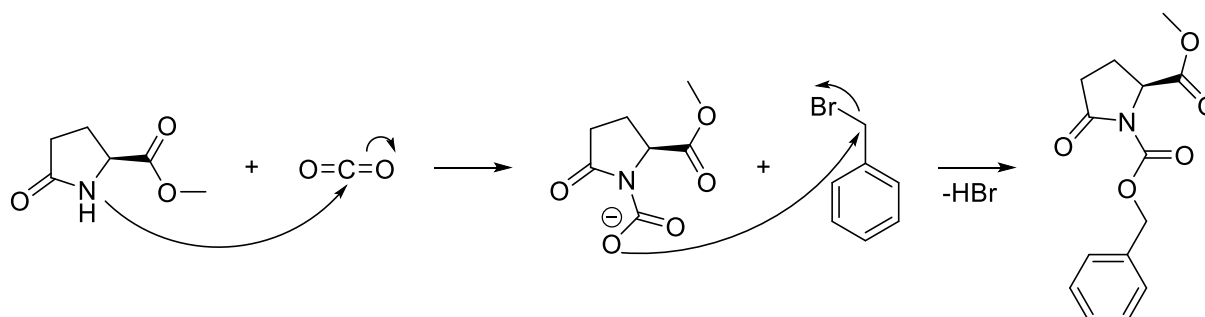
Figure 3: Reaction mechanism of the N-carboxy benzylation

In the mechanism illustrated by figure 3, the pyroglutamate ring stays closed and it thus undergoes no racemisation. In the first step, the free electron pair of the nitrogen attacks on the carbon atom of CO_2. This reaction takes place because the base activates the PGM and pulls the proton away. The electron pair on the negative oxygen will react in the next step with benzyl bromide in an S_N reaction.

This reaction will be followed by an ester amidation of the methyl N-carboxy benzyl pyroglutamate presented in figure 4.
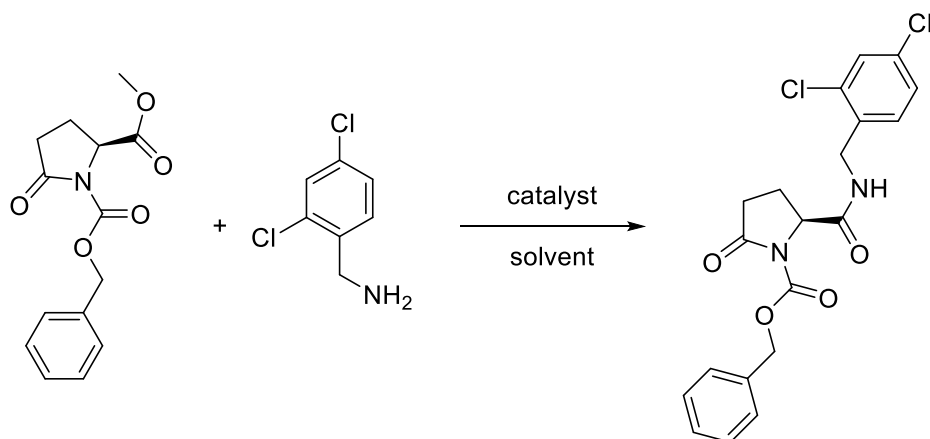
Figure 4: Step 2 Ester amidation of methyl N-carboxy benzyl pyroglutamate with 2,4-dichlorobenzylamine

Homerin et al. studied the ester amidation for similar molecules as shown in Figure 4 above. They achieved good results by using the Lewis acid $ZrCl_4$ as a catalyst in ACN at reflux temperature or in toluene at 90°C [12]. However, Homerin et al. did not use *N*-carboxyalkyl pyroglutamates for the ester amidation. This could have an effect on the activation of the reaction because there is a carboxylate bonded on the lactam group instead of an alkyl group. The expected mechanism for the ester amidation is shown in figure 5.
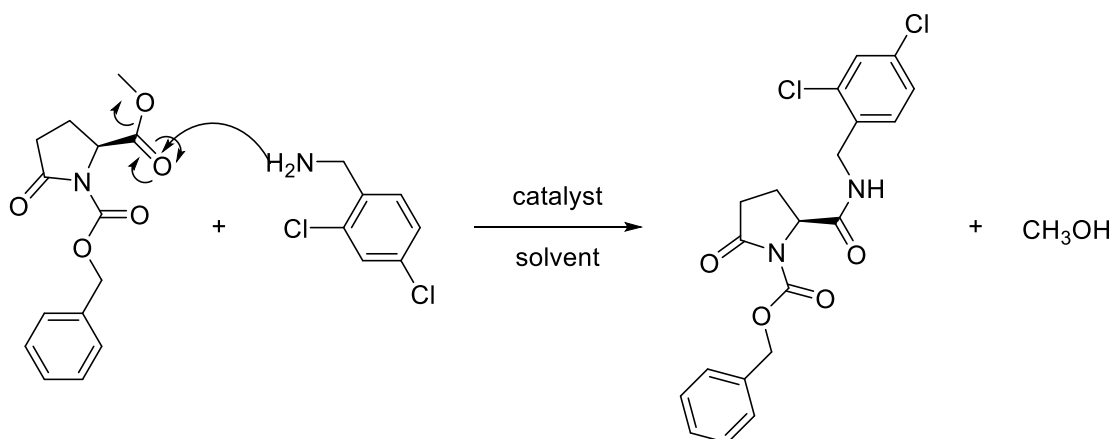
Figure 5: Expected reaction mechanism of the ester amidation

In the reaction mechanism illustrated by figure 5, the electron pair of the amine attacks on the partially positive carbon of the carbonyl group. This results a condensation reaction with methanol as a side product.

1.4.   Catalysts

Three catalysts will be investigated in this study. These are $ZrCl_4$, an ecocatalyst rich in calcium (Eco-Ca) and an ecocatalyst rich in iron (Eco-Fe). $ZrCl_4$ is a Lewis acid which is known for its catalytic activity in organic synthesis [12]. This catalyst works by complexing the oxygens present in the molecule such as the first molecule shown in figure 4. By complexing the oxygen atom of the carbonyl, the carbon becomes more positive because the electrons are pulled away from it. This causes

the electron pair of the amine to attack easier on the carbon of the carbonyl group as shown by figure 5. Lewis acid catalysts are thus interesting for organic synthesis because of their selectivity and mild reaction conditions used. These catalysts also have some disadvantages such as their moisture sensitivity. They deactivate quickly when they come in contact with water because they react faster with OH^-. Thus, the reaction must take place in a water free medium. They also cannot be recovered or reused at the end of the reaction [13].

On the other hand, ecocatalysts can be used as biosourced Lewis acids which are more eco-friendly and fit perfectly in the circular economy. These ecocatalysts come from metal tolerant plants such as *Lolium perenne* L., *Miscanthus x giganteus*, etc which have grown on metal contaminated soils. The contaminations of metals in the soil come from present or past industrial activities in the area where the plants are grown. The Eco-Fe originates from contaminated soils in Belgium and the Eco-Ca originates from contaminated soils in northern France. By ashing the plants, the metals can be concentrated. These metals are then chlorinated by treating them in HCl to obtain the metal chlorides, which serve as the biosourced Lewis acid catalysts. [14]. These ecocatalysts thus contain a variety of other metal chlorides but in smaller quantities. These work on the same way as $ZrCl_4$ but with other metal chlorides which could work together to possibly achieve better activation. The catalyst which gives the best results will be used for the kinetic experiments to then find the optimal temperature and concentration of both reagents of the ester amidation reaction. The exact composition of the ecocatalysts have been determined by using flame atomic absorption spectroscopy (FAAS) and X-ray spectroscopy.

1.5. Green solvents

The solvents which can be used for chemical reaction are of great importance since they are estimated to have an emission contribution of 60% of all industrial emissions and 30% of all volatile organic compounds (VOC's) [15]. The availability and manufacturing of the solvent is important but also the safety on human health and environment. Thus, solvents which: originate from renewable sources, have less emissions or are less hazardous can be classified as green solvents. However, there is no ideal solvent which can be used in every case and also satisfy all these specifications [16].

Homerin et al. tested ACN as a solvent for the both type of reactions shown in figure 2 and 4 [4] [12]. This solvent seems to be the best candidate if the 2 experiments need to be conducted in one flask. Nevertheless, the use of a green solvent also needs to be tested to see how it affects the reaction. Ethanol could be a possible solvent for the 2 reactions. However, since it is a PPS solvent, it could solvate the molecules too much which could slow the reaction down. It could also participate in other unwanted side reactions such as a transesterification for the second reaction. Ethanol is a green solvent because it can be made from renewable sources such as sugar containing feed, starchy feed materials or lignocellulosic materials [17]. Another possible solvent which could be used for the ester amidation is NBP because it is also a DAS solvent like ACN. NBP is also a greener solvent then ACN. Other solvents which are greener than ACN are 2-MeTHF and dimethyl carbonate.

The solvents that are used in the literature are DMF for the *N*-carboxy benzylation and toluene for the ester amidation. But because of their health hazards they will not be used in this study. The most important feature of a solvent is to serve as a reaction medium. Therefore, the reagents need to dissolve in it to increase reaction speed and yield. The solvation of reactive ions also needs to be minimized to make sure the molecules collide easier with each other. The reaction shown in figure 2 uses CO_2 as a reagent which is in a gas phase that must dissolve in the solution. The solubility of CO_2 increases with decreasing temperature and increasing pressure [18]. The pressure can be kept as high as possible and for the temperature, an optimal setting has to be found since a lower temperature could also slow the reaction down.

1.6. Temperature

The goal of this research is to optimize the two reactions shown in figure 2 and 4. To be able to optimize the reaction, the factors that could influence the reaction rate and yield have to be studied and the reaction temperature is one of those factors. The reaction rates usually increase with higher temperatures. This does not always mean that the yield of the product increases. For exothermic equilibrium reactions, the yield or conversion decreases with higher temperatures and the opposite is true for endothermic equilibrium reaction [19]. Since the reactions are irreversible, they will always progress near completion given enough time. The temperature effect of the reactions can be studied by following the conversion during the reaction. The Arrhenius law gives the relation between the temperature and reaction rate constant.

1.7. Type of amine

The type of amine used on the second step reaction could also have an effect on the yield and reaction rate. The first amine which will be studied is 2,4-dichlorobenzylamine. For the reaction on figure 4 to happen, the free electron pair on the nitrogen must attack on the carbonyl carbon of the methyl ester group. By changing this amine into a 2,4-dichloroaniline, the reaction would probably be slower since the NH_2 group is directly bonded to the aromatic ring with 2 chlorines in ortho and para position. The reason is that the -I - effect of the chlorines would make it harder for the electron pair to attack on the carbonyl carbon [20].

The opposite is true for when the chlorine groups are changed into methoxy groups. The methoxy group in para position has a +M – effect which pushes electrons more to the NH_2 group and therefore the electron pair is more likely to attack on the carbonyl carbon of the methyl ester group [20]. This will be studied by using 4 types of amines, namely: 2,4-dichloroaniline, 2,4-dichlorobenzylamine, 2,4-dimethoxybenzylamine and 2,4-dimethoxyaniline. In figure 6, these amines are shown in increasing electron pushing effect from left to right.
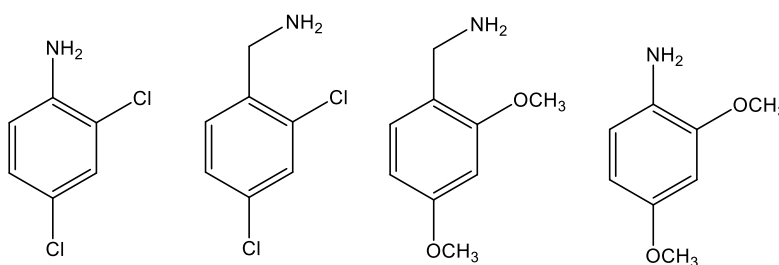
Figure 6: 2,4-substituted aromatic amines ordered in increasing electron pushing effect

1.8. Problem statement and project objective

The challenge for the first reaction shown in figure 3 is that the optimal temperature is not known for the use of a safer and more green solvent than the ones that are used in the literature. The safer

solvents which will be tested are ACN, dimethyl carbonate and 2-MeTHF. The objective is also to have an idea on how the temperature affects the reaction rate. The type of base, phase transfer agent and the reagents will not be investigated since these have already been studied in the literature.

The second reaction has not yet been reported in the literature. First, it is investigated if the proposed pathway is possible and if the obtained product is indeed the target molecule illustrated in figure 5. The optimal temperature, solvent and catalyst are researched. The types of catalyst and solvent which will be studied are those who have also been used in the literature for similar reactions. This will be done by also opting for green chemistry such as the use of ecocatalysts and solvents. Also, the temperature effect will be studied by conducting kinetic experiments. This involves following the concentration progression of the reagents during the reaction. Another factor that will be investigated is the use of differently substituted aromatic amines to see how the inductive and mesomere effects affect the reaction. Eventually the two reactions will be conducted in one flask to see if this is possible, how the reaction progresses and what the yield is. This could potentially reduce losses of intermediate reagents and the synthesis time because of omitted purification steps in between the two reactions.

2. MATERIALS AND METHODS

2.1. Materials

2.1.1. Chemicals

The starting materials of the *N*-carboxy benzylation illustrated in figure 1 were bought from chemical suppliers except for the methyl L-pyroglutamate (PGM). PGM is synthesized by the research group from pyroglutamic acid (PGA). This PGA is extracted from sugar beet molasses. Cesium carbonate (purity > 95%), tetrabutylammonium bromide (purity > 99%) and 2,4-dichlorobenzylamine (purity > 98%) were bought from TCI Europe n.v. Benzyl bromide was bought from Lancaster Synthesis and it had a purity of 99%. CO_2 was bought from Air Liquide (France) and its purity was 99.99%.

Chloroform-D was used as a solvent for the NMR analysis. It had trimethylsilane (0.03%) as an internal standard. This chloroform-D was supplied by Eurisotop and it had a deuterium percentage of 99.8 %. The ecocatalysts used for the ester amidation were produced by JUNIA ISA (agricultural, agri-food and environmental engineering school). The exact composition of the metals in the Eco-Fe and the Eco-Ca are shown in table 2.

Table 2: Composition of the ecocatalysts

catalyst		Cd (mg/kg)	Pb (mg/kg)	Zn (mg/kg)	Cu (mg/kg)	Fe (mg/kg)	K (mg/kg)	Na (mg/kg)	Ca (mg/kg)	Mg (mg/kg)
Eco-Ca	Mean	<0.4	7.9	37.4	4.7	77.1	64003.3	3707.4	6483.8	2270.2
	Standard deviation		1.7	1.1	0.3	25.5	7910.7	534.3	994.2	184.4
Eco-Fe	Mean	<0.4	7.2	51.2	4.8	361.1	46711.9	7611.3	5645.6	2554.1
	Standard deviation		1.7	5.6	0.4	196.7	9825.2	5438.3	2229.8	521.9

2.1.2. Experimental setup

The reaction illustrated in figure 1 was done in a round bottom flask of 100 mL. The flask was placed in a water bath on top of a hotplate to control the temperature. The temperature is measured by a temperature sensor. Furthermore, The mixture was stirred by using a magnetic stirrer at 500 rpm, and the CO_2 atmosphere in the flask was achieved by securing a balloon filled with CO_2 on top of the flask. The setup is illustrated in figure 7.
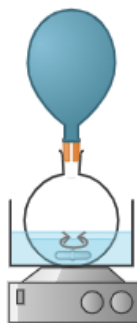
Figure 7: Experimental setup for the N-carboxy benzylation

In figure 7, an ice bath is added for experiments with temperatures of 0°C.

For the second reaction shown in figure 4, higher temperatures were needed. Thus, a round bottom flask of 100 mL was placed in an oil bath which was also placed on a heating plate. The temperature was controlled by a temperature sensor. On top of the flask, a condenser was placed to prevent vapor from escaping and thus to keep the volume constant in the batch reactor. The mixture was stirred with a magnetic stirrer at 250 rpm. This setup for the ester amidation is illustrated in figure 8.
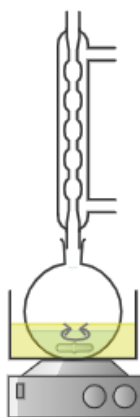
Figure 8: Experimental setup for the ester amidation

2.2.   Methods

2.2.1.   *N*-carboxy benzylation and ester amidation reaction

For the *N*-carboxy benzylation shown by figure 2, 3 equivalents of TBAB and cesium carbonate are added into a round bottom flask for all experiments. Then PGM is added together with 15 mL of solvent. The round bottom flask is then purged with CO_2 gas. Eventually, benzyl bromide is added, and the reaction mixture is stirred with a magnetic stirrer under a CO_2 atmosphere provided by the balloon as shown in figure 7. The solubility of CO_2 in ACN, 2-MeTHF and dimethyl carbonate are calculated by the ProPhyPlus program from ProSim. The thermodynamic model used for the

simulation of CO_2 solubility in these solutions is Predictive Soave-Redlich-Kwong (PSRK). The simulated solubility of the mentioned solvents is illustrated by figure 9.
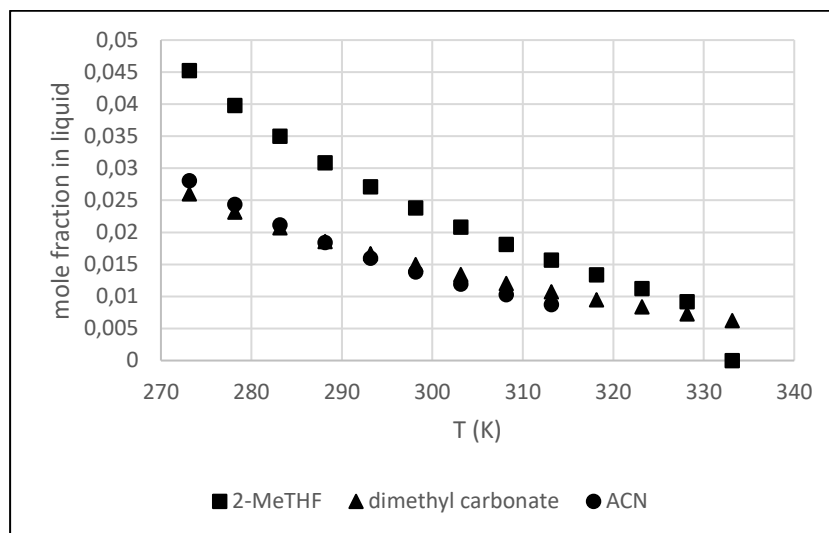
Figure 9: Solubility of CO2 in function of the temperature

In figure 9 the solubility of 2-MeTHF, dimethyl carbonate and ACN are shown. The calculations show that 2-MeTHF has the largest solubility of CO_2. ACN and dimethyl carbonate have similar solubilities.

For the ester amidation, 100 mg of ecocatalyst or 0.05 equivalents of $ZrCl_4$ are added to a round bottom flask. Then the methyl *N*-carboxy benzyl pyroglutamate is added together with the amine and 5 mL of solvent. The flask is then placed in a hot oil bath on the hotplate together with a magnetic stirrer. Finally, The condenser is secured on top of the flask as shown by figure 8.

2.2.2. Purification

Purification steps are needed after a reaction to separate the target molecule from the used solvents reagents and side products in the reaction mixture. For the step 1 reaction a vacuum filtration followed by a flash chromatography is necessary to isolate the product. This is a rapid separation technique which uses compressed air and small silica gel particles [21]. The flash chromatography that is used in this study is the CombiFlash R_f Teledyne isco. The pre-column and the column have silica gel particles of 0.04 - 0.063 mm supplied from Macherey-Nagel. The mobile phase consists of a non-polar and a polar solvent which are respectively *n*-heptane (99 % purity) and ethyl acetate (99.9 % purity) bought from Carlo Erba reagents. The fraction of these two solvents changes in time and transport different compounds based on their polarity through the column. The eluted compounds are recovered separately [22]. This purification step is needed after the first reaction to use the product in the next reaction.

For the step 2 reaction, purification can be accomplished by crystallization and vacuum filtration. This is a technique where the solid phase is separated from the solvent and other liquid side products [23]. When using ACN, the target molecule is soluble in it at higher temperatures and precipitates at lower temperatures. Thus, cooling crystallization can be used for the purification of the target molecule. If a better purification is necessary, a flash chromatography can be used

2.2.3. Analysis

There are a variety of analysis methods for organic compounds. The goal of the analysis during this study is to follow the progress of the reaction, to see what the purity is and to measure the yield obtained for each reaction. To check the progression of the reaction roughly, the presence of the reagents in the reaction mixture can be checked with thin layer chromatography (TLC). This is a quick and reliable technique to verify if the reaction is over. This analysis is based on chromatographic principles where there is a stationary phase and a mobile phase. A drop of each reagent together with the drop of the reaction mixture will be placed on the baseline of the TLC. The TLC can then be placed on a mobile phase which is a mixture of a polar and a non-polar solvent. The fraction of these 2 liquids determines how far the spots on the TLC travel. The spots can be looked at under a UV-light since all the compounds have an aromatic ring and absorb UV-light. Thus, the spots are dark, and the silica is slightly lightened up. After indicating the spots, the Rf value of each spot can be calculated by dividing the travel distance of a spot between the baseline and the solvent front [24].

The purity of the obtained product can be determined more precisely by proton or carbon nuclear magnetic resonance spectroscopy (^{1}H-NMR or ^{13}C-NMR). This is a technique to determine the molecular structure of a molecule. A strong magnetic field is utilized in this technique to measure the spinning nuclei of the hydrogen or carbon atoms [25]. A sample is placed in an NMR tube together with chloroform-D as a solvent. This is then placed in the NMR for analysis. The NMR used in this study is the Varian 400 MHz NMR. A spectrum is generated with this technique that shows peaks that correspond to the hydrogens or carbons in the molecules present in the sample. This method can be used to follow the conversion of the reagents during the reaction by comparing the area of a peak of the target molecule and reagent. This method will thus be used to determine the kinetic parameters of the step 1 and 2 reaction.

To determine if the reaction undergoes racemisation, the molecules are analysed with the Anton Paar MCP 5100 polarimeter. Polarimetry is the measurement of optical rotation of a medium. In this analysis technique, the light passes through a polarizer. Here the light is filtered into waves that are aligned in one direction. This light then passes through a tube, which is usually 1 dm long, with the medium to be studied [26]. The medium here is a solution of 5 mg of target molecule dissolved in 1 mL of dimethyl sulfoxide (DMSO). After the light passes through the tube, it then passes through another polarizer which is rotated at another angle until the light can pass through a slit which then goes to the sensor. This angle will be zero if the medium is not optically active [26]. A visual representation of this is illustrated in figure 10.
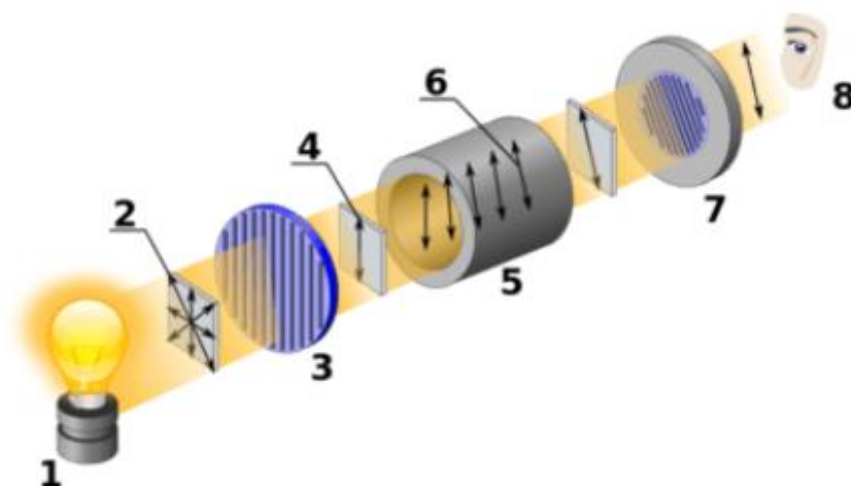

Figure 10: Basic diagram of a polarimeter [26]

Biot's law states that the angle of rotation is proportional to the length of the tube and the concentration of the compound. The proportionality constant is called the optical rotation and this is dependent on the wavelength and the temperature. This relation is shown in eq. (1).

$$\alpha = [\alpha]T \cdot l \cdot C \tag{1}$$

In eq. (1), $[\alpha]T$ is the optical rotation, l is the length of the sample tube and C is the concentration of the compound in the medium. Eq. (2) can be used to determine the $[\alpha]_\lambda^T$ value at a certain wavelength (λ) and temperature (T).
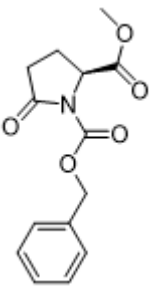
$$[\alpha]_\lambda^T = \frac{V}{l\,C}\alpha \tag{2}$$
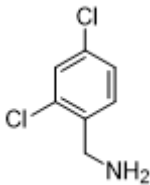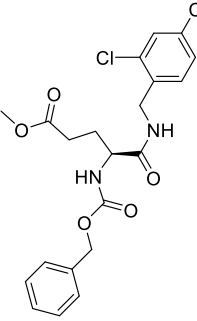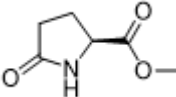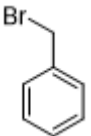
In eq. (2), V is the volume in mL, l is the length of the sample tube in dm, C is the concentration in g/mL and α is the observed angle in °. If the $[\alpha]_\lambda^T$ value is negative, then it means that the enantiomers in the solution rotate the light in a counter-clockwise direction. This is called levorotatory (L). If the $[\alpha]_\lambda^T$ value is positive, then it means that the enantiomers rotate the light in a clockwise direction and this is called dextrorotatory (D). If the solution contains a racemic mixture of a compound with a 50:50 mixture of enantiomers, then the $[\alpha]_\lambda^T$ value will be zero, which means that the solution is not optically active. The light rotation of L- and D-isomers cancel each other [27].

The last analysis method that is used is the melting point analysis with the OptiMelt Automated Melting Point System from Stanford Research Systems. Here, a purified and dry sample of the product is placed in a melting point analysis capillary tube. The tube is then placed into the machine which performs the measurement automatically. This analysis method is not only used to determine the melting point of a compound but also to have an idea on the purity. If the temperature range of the melting point is too large, then this means that the product is not pure enough and thus requires a better purification [28].

2.2.4. Kinetic experiments

The reagents and products of the first and the second reaction will be named by letters as a simplification. Table 3 below shows what letter belongs to which molecule.

Table 3: Letter code for the molecules

A	B	C	D	E	F

The reaction behaviour due to temperature changes can be studied by determining the kinetic parameters for each catalyst. This can be modelled by the Arrhenius equation shown in eq. (3).

$$k = k_0 e^{\frac{-E_a}{RT}} \tag{3}$$

the reaction rate constant is displayed by k, k_0 is the pre-exponential factor, E_a is the activation energy, R is the molar gas constant and T is the temperature. Once these kinetic parameters are known, the Arrhenius equation can be used as a model for the temperature effect on the reaction. First the order of the reaction has to be determined. The general equation for the reaction rate of the reaction in figure 4 is shown by eq. (4).

$$\frac{-dC_A}{dt} = \frac{-dC_B}{dt} = -r_A = k \, C_A^n \, C_B^m \tag{4}$$

In eq. (4), r displays the reaction rate, k is the reaction rate constant, C_A and C_B are respectively the concentration of the first and second reagent in figure 4. The letters n and m represent the exponents which give more information about how the two reagents each affect the reaction rate. The overall order of this reaction should be two since this is a bimolecular reaction, thus first order for both A and B [29].

To verify if A and B are both first order, the exponents were determined. This is done by adding a large excess of one reagent to assume this stays constant during the reaction. The concentration of one reagent should be at least ten times larger than the other to assume it stays constant during the reaction. The rate equation shown by eq. (4) simplifies to eq. (5) below when C_B is much larger than C_A.

$$-r_A = k' \, C_A^n \tag{5}$$

This equation can be used to verify if n is first order. This can be done experimentally by using the integral method. The data points can be fitted for first and second order assumption, to see which assumption has the best fit on the obtained data. For a first order reaction eq. (6) would yield a linear plot.

$$ln(\frac{C_{A0}}{C_A}) = kt \tag{6}$$

In eq. (6), C_A displays the concentration of the first reagent for the step 2 reaction and t displays the reaction time. Eq. (7) can be used for a second order assumption.

$$\frac{1}{C_A} = kt + \frac{1}{C_{A0}} \tag{7}$$

The equation for another order can be derived from the general form and with trial and error for the exponent n, a fit can be found that has the largest R^2 value. The general form is shown in eq. (8).

$$\frac{-dC}{dt} = kC^n \tag{8}$$

After determining the order of the reaction, the reaction rate constant was determined experimentally. For a bimolecular second order reaction where both A and B are equimolar, the reaction rate constant can be determined by fitting the data in a linear plot represented by eq. (9).

$$\frac{1}{C_B} = kt + \frac{1}{C_{B0}} \, or \, \frac{1}{C_A} = kt + \frac{1}{C_{A0}} \tag{9}$$

Once the reaction order and the reaction rate constant k for various temperatures were known, the activation energy was calculated by using eq. (10).

$$ln(\frac{k_1}{k_2}) = \frac{E_a}{R}(\frac{1}{T1} - \frac{1}{T2}) \tag{10}$$

The activation energy can be determined experimentally by determining the reaction rate constant for different temperatures and then by plotting the ln(k) vs 1/T graph. The slope of the trendline displays -E_a/R [19]. The pre-exponential factor k_0, was then calculated with eq. (3). This method will be used for both reactions.

3.1. Step 1: *N*-carboxy benzylation reaction

3.1.1. Concentration effect

First, the order of the reaction is determined to understand how the concentration of the reagents affect the reaction rate. The difficulty for this reaction is that the concentration of CO_2 in the reaction mixture cannot be measured or controlled easily. The concentration of CO_2 in the reaction mixture is not measured during the reaction because there was no precise dosing of CO_2 gas in the round bottom flask. At lower temperatures such as 0°C the concentration of CO_2 could be assumed constant and close to the concentration found with the simulation program ProPhyPlus illustrated in figure 9. But, at higher temperatures the reaction will be faster and thus, the rate limiting step could become the diffusion of CO_2 in the solution. This hinders the concentration of CO_2 to reach the equilibrium concentration. The temperature at which the diffusion will become the rate limiting step will be determined by the temperature effect experiments at section 3.1.2. The first reaction conditions that were tested to investigate the concentration effect of reagent D and F are shown in table 4.

Table 4: Reaction conditions of concentration effect experiments

Experiment	solvent	T (°C)	C_{D0} (M)	C_{F0} (M)	Molar ratio (D:F)
1	ACN	21	0.239	0.023	10:1
2	ACN	21	0.049	0.466	1:10

These experiments resulted in the conversion versus time graph illustrated in figure 11.
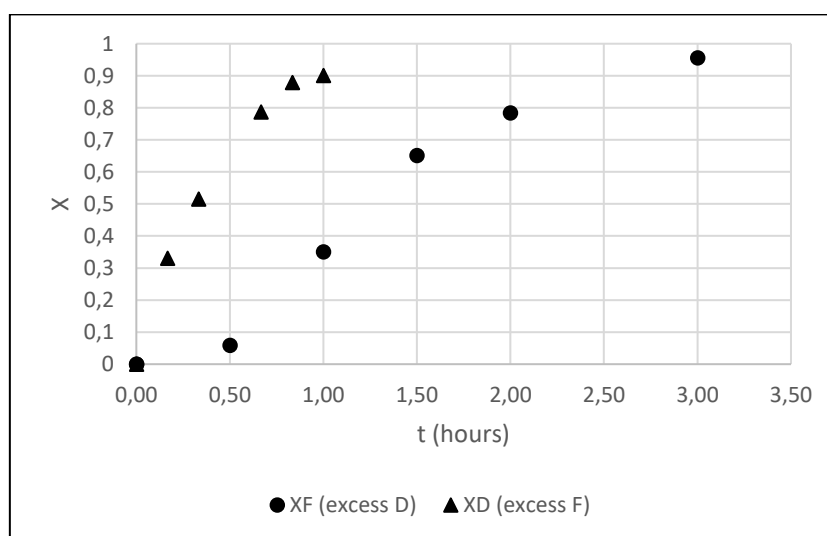
Figure 11: Concentration effect of reagents for the N-carboxy benzylation

Figure 11 shows that when a small amount of reagent D is added, the reaction rate is much faster than when a small amount of F is added. This is logical since the intermediate formed from the reaction of PGM and CO_2 has to react with the benzyl bromide (reagent F). When a small amount of benzyl bromide is added, the chances of the intermediate colliding with the benzyl bromide are smaller and thus, the reaction becomes slower. By adding an excess of benzyl bromide, the reaction will go faster because there is a larger chance of collisions between the intermediate and benzyl bromide.

The order of reagent D and F can now be determined by fitting the data in zeroth, first or second order assumption. For experiment 1, this resulted in the following graph illustrated in figure 12.
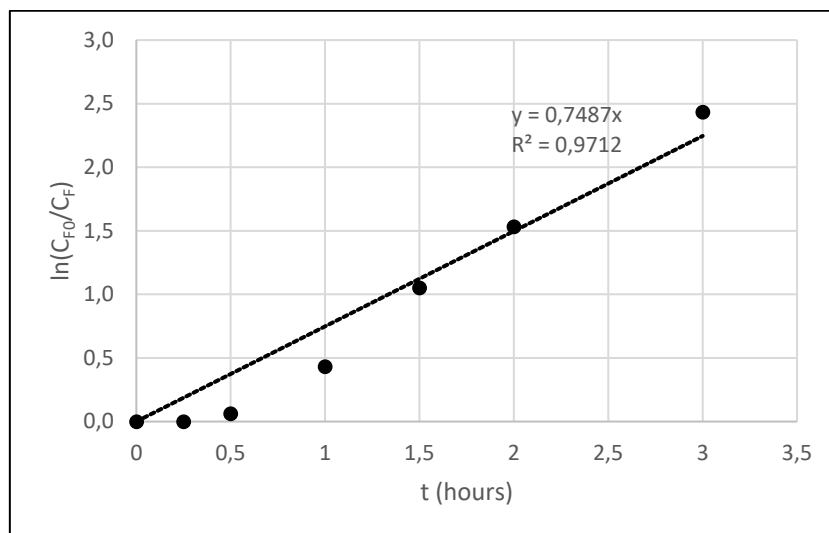
Figure 12: First order assumption for reagent F

For experiment 1, a first order assumption, illustrated in figure 12, had the best fit on the data. It is noticeable from the R^2-value that the fit does not seem ideal. The reason is that reagent F seemed to start reacting after 15 minutes. From the reaction mechanism in figure 3, it is clear that in the beginning not much intermediate is formed for reagent F to react with. The induction time for the conversion of this reagent is thus 15 minutes. After 30 minutes the data also seem to fit better in a first order assumption. Therefore, the following graph illustrated in figure 13 is made, where the first two data points with conversion zero are removed.
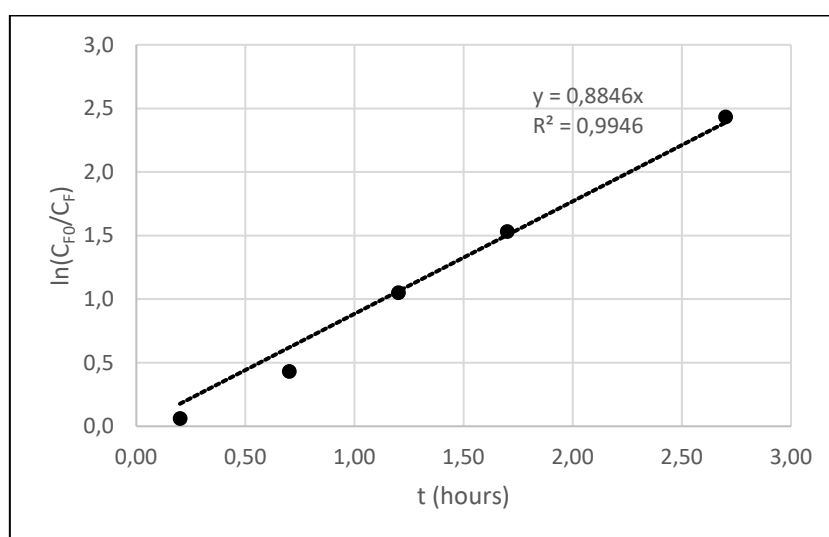
Figure 13: Modified first order assumption for reagent F

In Figure 13, the data fits better in a first order assumption when an induction time of 15 minutes is considered. Thus, reagent F is first order with reaction rate constant k in 1/hours. The rate equation of this experiment is shown by eq. (11).

$$-r_F = 0.88\, C_F \tag{11}$$

Next, the best fit obtained for the data of experiment 2 is illustrated by figure 14.
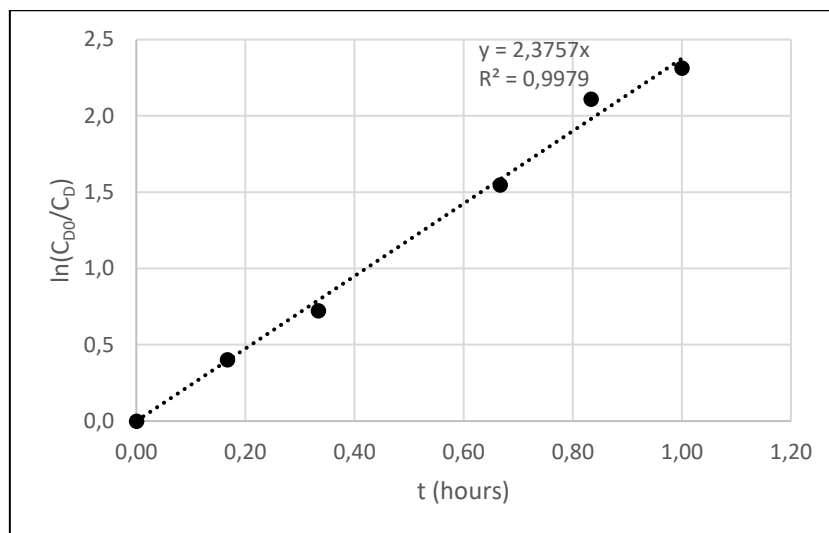
Figure 14: First order assumption for reagent D

In figure 14, the data of experiment 2 fit almost perfectly in a first order assumption. Thus, reagent D is also first order with reaction rate constant k in 1/hours. The rate equation of this experiment can be written as eq. (12).

$$-r_D = 2.38 \, C_D \tag{12}$$

The overall order of the reaction is not determined since the concentration CO_2 could not be followed.

The rate equation where the concentration effect of CO_2 is in the reaction rate constant is described by eq. (13).

$$-r = k' \, C_D \, C_F \tag{13}$$

The reaction rate constant k' in eq. (13) is the actual reaction rate constant k multiplied by C_E^n. This will be verified by one of the temperature effect experiments.

3.1.2. Temperature effect

To see how the temperature affects the reaction rate, 4 experiments are conducted with 4 different temperatures. The reaction conditions of these experiments are shown in Table 5.

Table 5: Reaction conditions of the temperature effect experiments

experiment	solvent	T (°C)	C_{D0} (M)	C_{F0} (M)	Molar ratio (D:F)
1	ACN	0	0.472	0.512	1:1
2	ACN	21	0.237	0.233	1:1
3	ACN	30	0.2412	0.233	1:1
4	ACN	40	0.2445	0.233	1:1

These experiments resulted in the conversion versus time graph illustrated by figure 15.
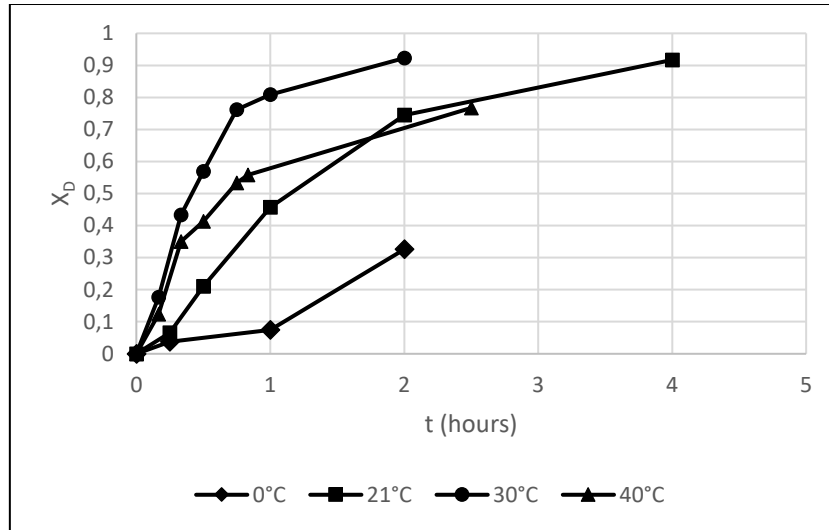
Figure 15: Temperature effect on the N-carboxy benzylation reaction. Data points are connected for guidance of the eye

Figure 15 shows that when the temperature increases until 30°C the reaction rate is higher. Thus, the optimal temperature found for this reaction lays around 30°C. This also means that the diffusion of CO_2 in the reaction mixture becomes the rate limiting step at a temperature between 20°C and 40°C. When the temperature is set at 40°C, there is a noticeable decrease in reaction rate. The reason could be that at higher temperatures the concentration of CO_2 in the reaction mixture decreases and this seemed more important at a temperature of 40°C. The reaction itself gets faster but less CO_2 diffuses in the reaction mixture at 40°C. Thus, at temperatures above 30°C the reaction could be much faster than the supply of CO_2 in the solution, which is observed when the temperature was set at 40°C.

To validate eq. (13) from the concentration effect experiments, the second order assumption is tested, derived from the general equation shown by eq. (8) for $C_{F0} \neq C_{D0}$, for experiment 3 at 30°C. Note here that for experiment 3, C_{F0} is almost equal to C_{D0}. But, due to the induction time the difference between the concentration grows quickly after the reaction starts. The equation for the second order assumption is shown by eq. (14).

$$(C_{F0} - C_{D0})kt = \ln \frac{C_F C_{D0}}{C_{F0} C_D} \tag{14}$$

The data of experiment 3 can now be fitted in the graph of $\ln \frac{C_F C_{D0}}{C_{F0} C_D}$ in function of the time illustrated in figure 17.
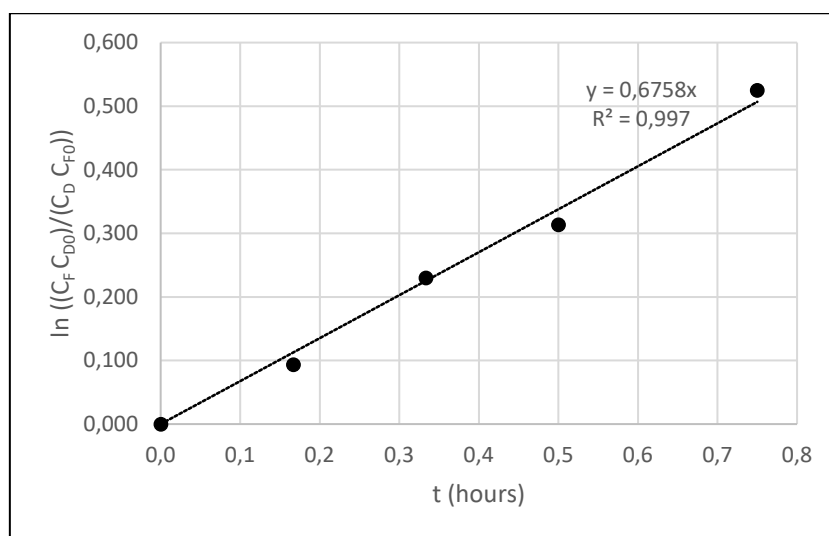
Figure 16: Second order assumption of the N-carboxy benzylation at 30°C

Figure 16 shows that there is a good fit for the second order assumption. This means that equation (13) is correct and for this experiment at 30°C eq. (13) can be written into eq. (15). The slope of the graph is equal to $(C_{F0} - C_{D0})k$. C_{F0} and C_{D0} is taken after an induction time of 15 minutes where both reagents are reacting.

$$-r = 23.1 \, C_D \, C_F \tag{15}$$

3.1.3. Solvent effect

2 other solvents were tested in 2 experiments with the reaction conditions shown by table 6 below.

Table 6: Reaction conditions of solvent effect experiments

Experiment	solvent	T (°C)	C_{D0} (M)	C_{F0} (M)	Molar ratio (D:F)
5	2-MeTHF	30	0.242	0.233	1:1
6	Dimethyl carbonate	30	0.2397	0.233	1:1

The target molecule was not obtained in these two experiments. This means that these solvents will also not be tested for the ester amidation. The solvent has to work for both reactions in order to do the 2 reactions in one flask. ACN works the best for this reaction and will thus be further utilized for the ester amidation.

3.1.4. Optimal reaction conditions

The yield for the *N*-carboxy benzylation is now measured with the best reaction conditions as shown in table 7.

Experiment	solvent	T (°C)	C_{D0} (M)	C_{F0} (M)	Molar ratio (A:B)
7	ACN	30	0.235	0.256	1:1.1

For this reaction the conversion was not followed. The yield after purification by flash chromatography was calculated from this experiment and it was equal to 73.4%. This is lower than the yield of 98% found in the literature. This could be due to losses during filtration and also during the purification step. It is possible that some product is also left behind in the column of the flash chromatography. Another experiment was conducted with the same conditions as Homerin et al. used. These reaction conditions are shown in table 8.

Table 8: Reaction conditions from the literature

Experiment	solvent	T (°C)	C_{D0} (M)	C_{F0} (M)	Molar ratio (A:B)
8	ACN	21	0.473	0.512	1:1.1

The yield obtained from this reaction is 55.2% which is even lower than the experiment at 30°C. Thus, a temperature of around 30°C seems to be the optimal temperature for this reaction.

3.1.5. Repetition experiments

Two repetition experiments were done for experiment three and four at 30°C and 40°C. This resulted in the conversion versus time graph illustrated in figure 17.

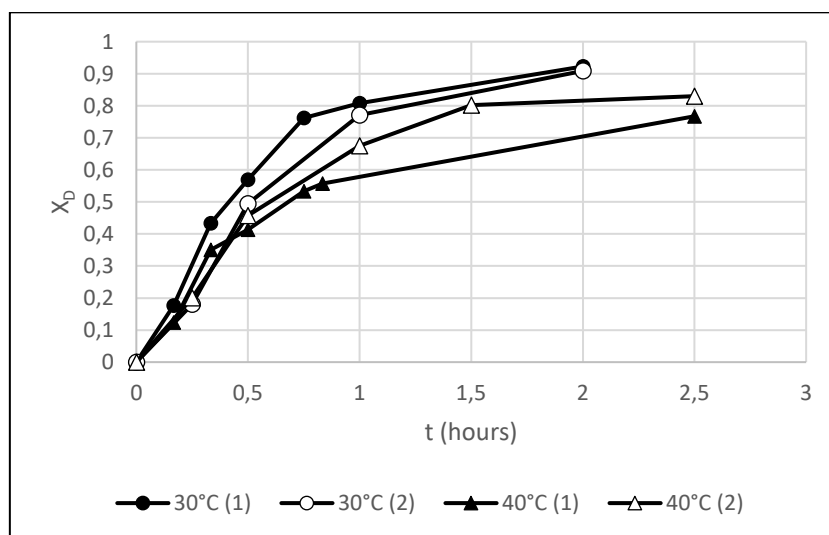*Figure 17: Duplicate experiments at 30 and 40°C. Data points are connected for guidance of the eye*

Figure 17 shows that there is some deviation for the repetition experiments, but they show the same effect as the original experiments. Both experiments at 40°C progressed slower than the experiments at 30°C. The average standard deviation between the conversions of the experiments at 30°C was 0.0296.

For 40°C the average standard deviation was 0.0528. The larger standard deviation for 40°C could be explained by the larger variation of CO_2 concentration in the solution due to the reaction being faster than the diffusion of CO_2 in the reaction mixture.

3.2.   Step 2: ester amidation reaction

3.2.1.   Obtained molecule

The expected molecule was not obtained when conducting the reaction illustrated by figure 3. Instead, although the amidation reaction was achieved, the 5-membered ring opened during the reaction. This reaction is illustrated by figure 18.
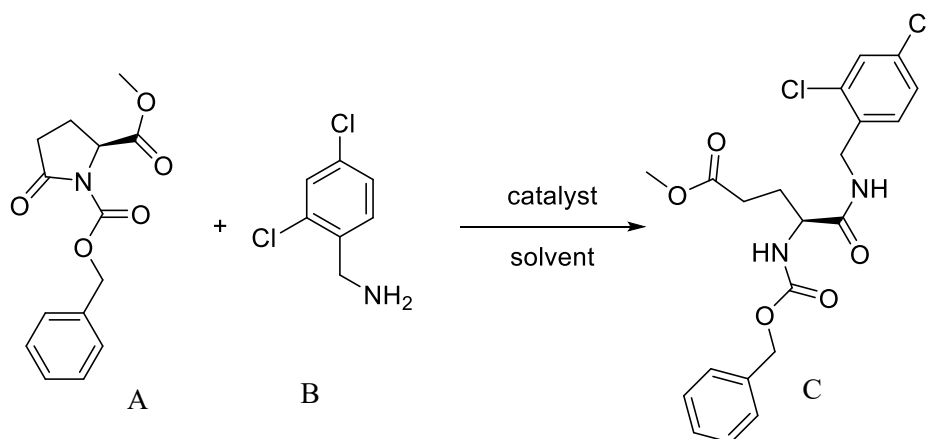
Figure 18: Obtained molecule from the ester amidation

The opened ring structure illustrated in figure 18 was not expected because in the study of Homerin et al. and Dufrénoy et al. the ester amidation of all their studied substituted pyroglutamates resulted in a closed ring structure [12], [30]. Thus, the possible reason why an opened ring molecule is obtained is because there is a carboxyl group present on PGM which was not previously investigated in the literature and since this is the only structural difference with previously studied pyroglutamates. This could cause the methanol side product to attack on the carbonyl carbon of the pyrrolidine-2-one ring. The methanol could also be activated due to the Lewis acid catalyst to the form of $(CH_3O^-)_4Zr^{4+}$. This will be verified by looking into synthetic alternative to achieve the closed ring target compound in the next section.

3.2.2.   Synthetic alternative to access closed ring target compound

The first experiment to try and achieve the closed ring compound is by conducting the ester amidation without any catalyst. This reaction took 30 hours to reach a conversion of 92.2%, which was expected because no catalyst was used. However, this experiment still resulted in the opened ring structure (compound C, figure 18). Thus, activation of methanol with the Lewis acid catalyst was not responsible for the ring opening reaction.

In another experiment, L-*tert*-butyl *N*-carboxy benzyl pyroglutamate (compound G, figure 19) was used as reagent which has a bulky ester group. This reaction is illustrated in figure 20.
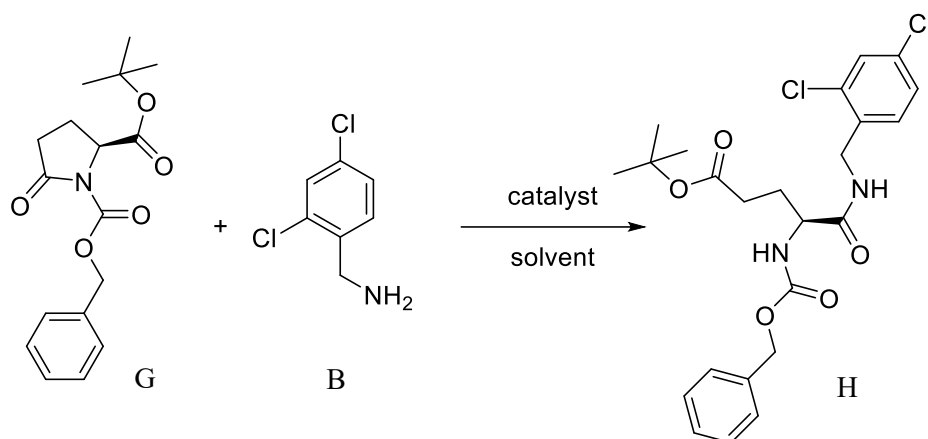
Figure 19: Ester amidation with tert-butyl ester

For the reaction illustrated in figure 19, the obtained molecule was also the opened ring compound with a *tert*-butyl ester group instead of methyl (compound H, figure 19). Thus, the ring opening reaction still occurred even with the bulky *tert*-butyl ester group.

3.2.3. Stereochemistry of obtained compounds

The optical activity is measured for the methyl *N*-carboxy benzyl L-pyroglutamate A and the opened ring compounds C and H. The $[\alpha]_\lambda^T$ at 25°C and wavelength of 365 nm and 589 nm are shown in table 9.

Table 9: Optical activity of obtained compounds

molecule	Wavelength (nm)	T (°C)	C (g/mL)	V (mL)	l (dm)	α (°)	$[\alpha]_\lambda^T$
A	365	25	0.005	1	1	-0.281	-56.2
	589	25	0.005	1	1	-0.135	-27
C	365	25	0.005	1	1	-0.161	-32.2
	589	25	0.005	1	1	-0.061	-12.2
H	365	25	0.005	1	1	-0.157	-31.4
	589	25	0.005	1	1	-0.063	-12.6

Table 9 shows that all the obtained molecules have a negative $[\alpha]_\lambda^T$ value which means that they are all L-enantiomers. This means that the studied reactions undergo no racemization.

3.2.4. Catalyst effect

Three experiments were conducted with three different catalysts. The exact reaction conditions of these experiments are presented in table 10.

Table 10: Reaction condition of catalyst effect experiments

Experiment	Catalyst	solvent	T (°C)	C_{A0} (M)	C_{B0} (M)	Molar ratio (A:B)
9	Eco-Ca	ACN	83 (reflux)	0.368	0.361	1:1
10	$ZrCl_4$	ACN	83 (reflux)	0.387	0.361	1:1
11	Eco-Fe	ACN	83 (reflux)	0.425	0.361	1:1

For these experiments the conversion was followed during the reaction. This results in the following conversion versus time graph illustrated in figure 20.
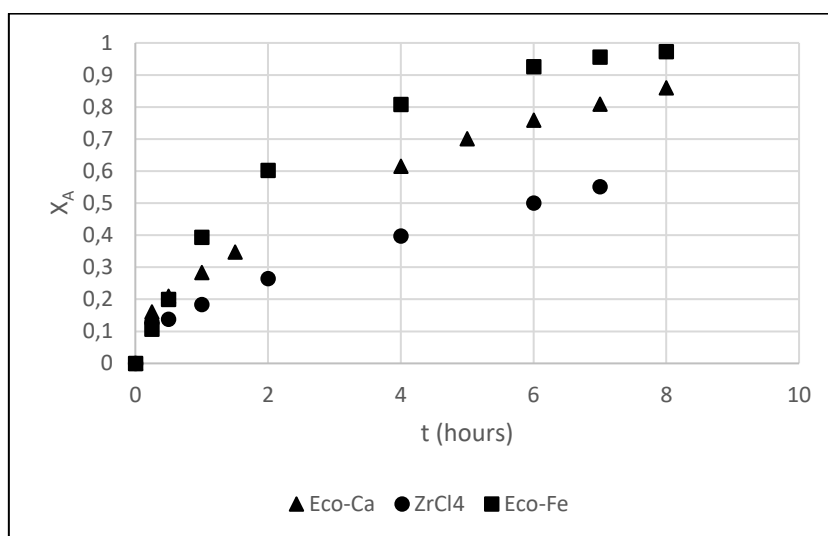

Figure 20: Conversion of A vs time graph of catalyst experiments

The conversion versus time graph illustrated by figure 20 shows the difference in reaction rate for the three catalysts. The Eco-Fe shows the best results. The traditional Lewis acid catalyst $ZrCl_4$ has the slowest reaction rate compared to the 2 ecocatalysts. This means that other metal chlorides in the ecocatalyst had a better effect on the activation of the carbonyl carbon which resulted in a larger reaction rate. The Eco-Fe reached near completion after 6 hours. Thus, this catalyst was used for further investigation on the concentration and temperature effect.

3.2.5. Concentration effect

In order to determine the concentration effect, the rate equation and the order of the reaction have to be determined. First, the order of the reaction is determined. As explained in 2.2.4 an excess of 1 of the two reagents is added to determine the reaction order of reagent A and B. This was done in two experiments. The reaction conditions of the experiments are shown in Table 11.

Table 11: Conditions for reaction order experiments

Experiment	Catalyst	Solvent	T (°C)	C_{A0} (M)	C_{B0} (M)	Molar ratio (A:B)
12	Eco-Fe	ACN	83 (reflux)	0.040	0.361	1:10
13	Eco-Fe	ACN	83 (reflux)	0.360	0.036	10:1

The experiments shown in table 11 resulted in the following conversion versus time graph illustrated by figure 21.
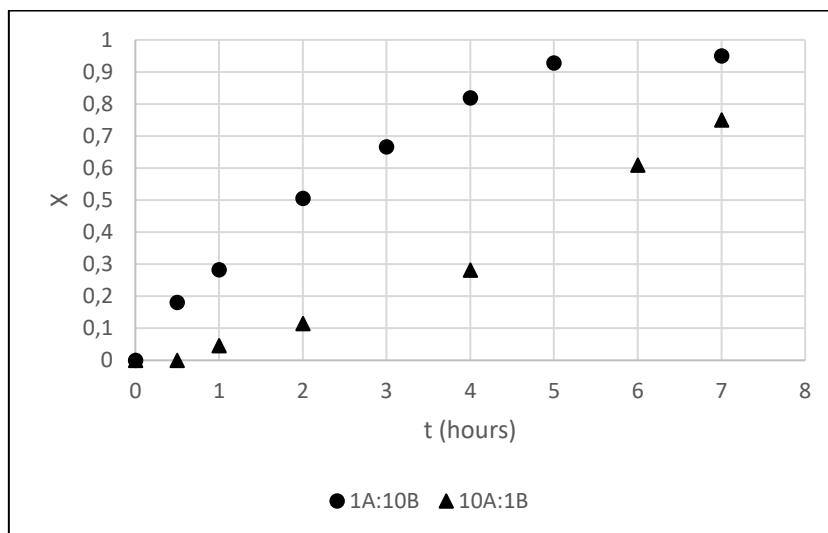
Figure 21: Conversion vs time graph for experiment 4 (X_A followed) and experiment 5 (X_B followed)

The conversion of reagent A and B were followed for respectively experiment 12 and 13 in figure 21. This figure shows that the reaction progressed faster when an excess of reagent B was added. Therefore, the reaction rate seems to be more affected by reagent A. For experiment 4, a first order assumption had the best fit on the data. The graph of the first order assumption for reagent A is illustrated in figure 22.
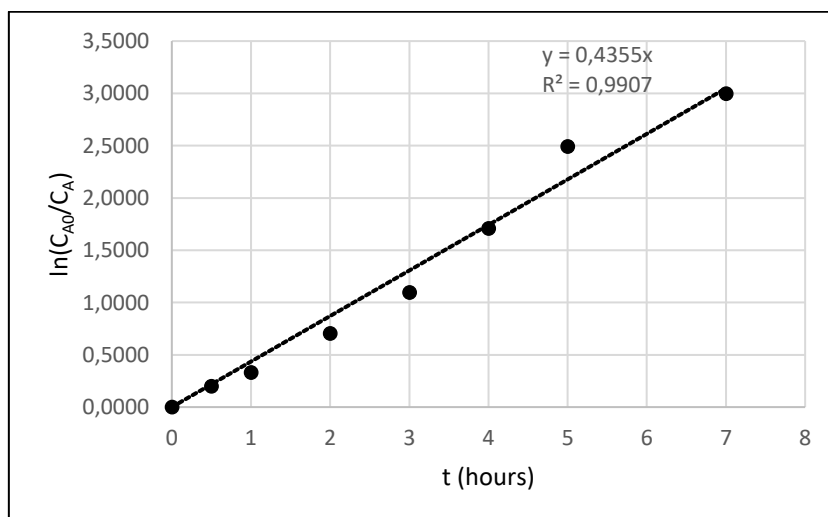
Figure 22: First order assumption for experiment 4

The graph illustrated in figure 22 shows the linear fit on the $\ln(C_{A0}/C_A)$ vs t graph. The slope of this equation represents the reaction rate constant k in 1/hours. The rate equation when an excess of B is added thus has the form shown by eq. (16).

$$-r_A = 0.44\ C_A \qquad (16)$$

The best fit on the data for experiment 5 is illustrated in figure 23 below.
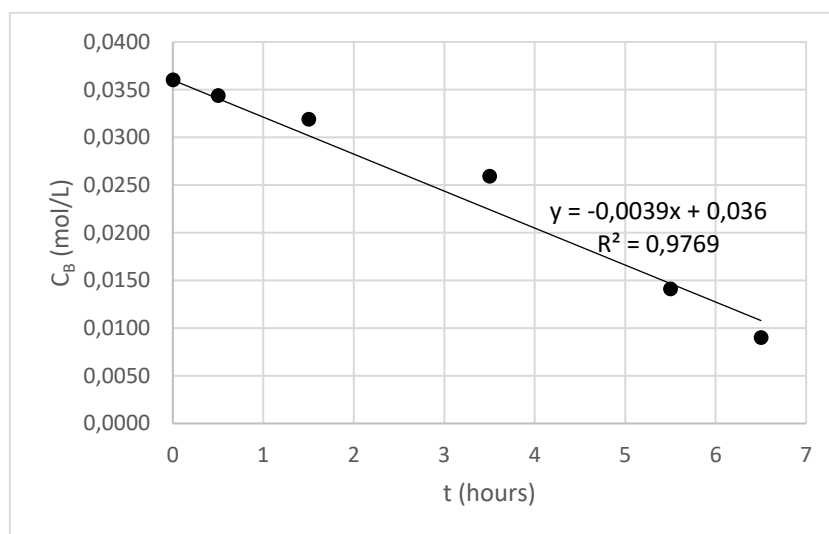
Figure 23: Zeroth order assumption for experiment 5

A zeroth order assumption has the best fit on the data of experiment 5 as illustrated in figure 23. However, a negative order has a better fit on this reaction but it is not logical because this would mean that the concentration of B is inversely proportional to the reaction rate. Larger orders than zero gave lower R² values. An order of zero is thus more logical and this means that the activation of reagent A by the Lewis acid catalyst could be the rate limiting step. The equation in the graph illustrated by figure 23 has a general form shown by eq. (17).

$$C_B = -kt + C_{B0} \qquad (17)$$

Thus, the overall rate equation of the ester amidation has the form of eq. (18).

$$-r_A = k\ C_A^1 C_B^0 = k\ C_A \qquad (18)$$

This was not expected since one molecule of A had to react with one molecule of B. The hypothesis was that this reaction would be a bimolecular reaction of second order, both first order in A and B. The rate equation shown by eq. (18) shows that only the concentration of reagent A affects the reaction rate. This means that the larger the concentration of reagent A is, the faster the reaction progresses. Thus, by adding an excess of reagent A, or by reducing the volume, the reaction will progress faster.

3.2.6. Temperature effect

To determine the temperature effect, four experiments were conducted on different temperature levels. The reaction conditions of these experiments are shown in table 12.

Experiment	Catalyst	Solvent	T (°C)	C_{A0} (M)	C_{B0} (M)	Molar ratio (A:B)
11	Eco-Fe	ACN	83 (reflux)	0.426	0.361	1:1
14	Eco-Fe	ACN	80	0.370	0.361	1:1
15	Eco-Fe	ACN	75	0.370	0.361	1:1
16	Eco-Fe	ACN	70	0.400	0.361	1:1

The results of these experiments are shown in the conversion versus time graph illustrated by figure 24.
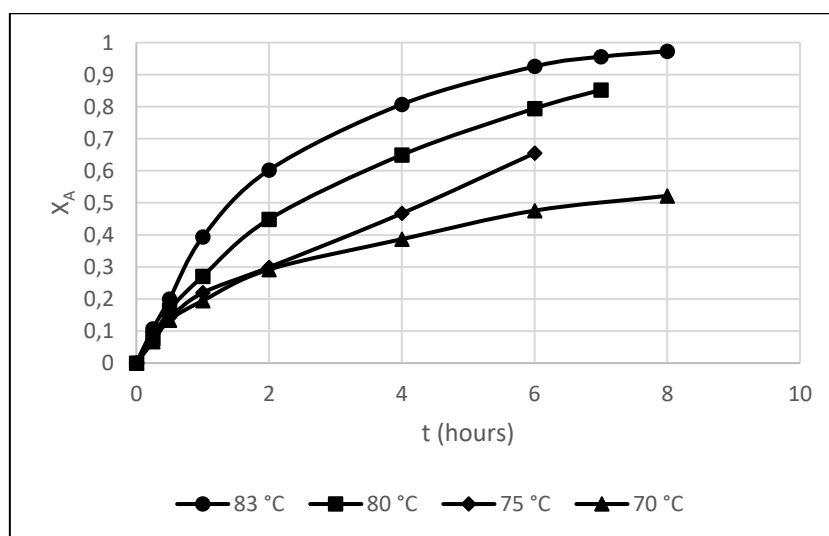
Figure 24: X_A vs t graph for the temperature effect experiments. Data points are connected for guidance of the eye

Figure 24 shows that when the temperature increases, the progression of the reaction increases. This is expected since the amount of molecule-molecule collisions increase with increasing temperatures.

Now, a model can be made for the temperature effect of this reaction by an Arrhenius-type relationship. From eq. (10) the ln(k) vs 1/T graph can be made. This is illustrated in figure 25.

Figure 25: Ln(k) vs 1/T graph for the temperature effect experiments

In figure 25 a linear equation is obtained. The slope of this equation represents E_a/R, thus E_a equals $108 \cdot 10^3$ J/mol. The intercept of the equation displays $\frac{-E_a}{RT}$. Thus k_0 can be calculated from eq. (3), which results in eq. (19).

$$k_0 = e^{\frac{-E_a}{RT}} = e^{(35.672)} = 2.98 \cdot 10^{15} \qquad (19)$$

3.2.7. Optimal reaction conditions
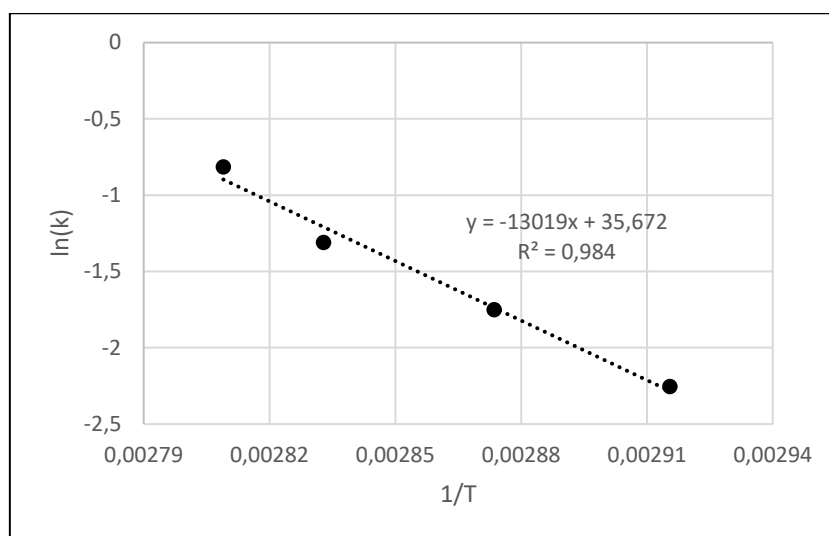
The yield of the ester amidation will be calculated with the best reaction conditions found. The optimal reaction conditions which were tested are shown in table 13.

Table 13: Optimal reaction conditions ester amidation

Experiment	Catalyst	Solvent	T (°C)	C_{A0} (M)	C_{B0} (M)	Molar ratio (A:B)
17	Eco-Fe	ACN	83 (reflux)	0.426	0.361	1:1

The product obtained in this reaction had a conversion of 95.6 % of opened ring product and it was purified using a flash chromatography. The final yield of the isolated product was 64.3%. Some losses could have occurred during the purification with the Flash chromatography.

3.2.8. Amine electronic effect

For the electronic effect on the amine, only the 2,4-dimethoxybenzylamine and 2,4-dichlorobenzylamine were tested because of their availability in the lab. The reaction conditions in which this amine was tested are shown by table 14.

Table 14: Reaction conditions of amine electronic effect experiments

Experiment	Amine	Catalyst	Solvent	T (°C)	C_{A0} (M)	C_{B0} (M)	Molar ratio (A:B)
18	2,4-dimethoxybenzylamine	$ZrCl_4$	ACN	83 (reflux)	0.368	0.361	1:1
10	2,4-dichlorobenzylamine	$ZrCl_4$	ACN	83 (reflux)	0.387	0.361	1:1

The experiments were done with 0.05 equivalent of $ZrCl_4$ because the Eco-Fe was not available anymore. The progress of the reaction from experiment 18 and 10 are illustrated in figure 26. The conversion of reagent A is shown in function of the reaction time.
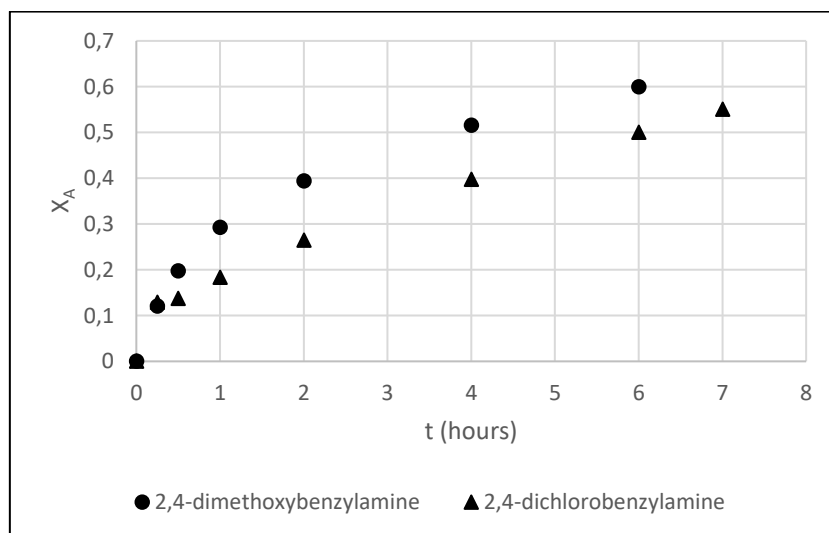
Figure 26: Conversion vs time for the amine electronic effect

Figure 26 shows that the reaction progresses faster for the 2,4-dimethoxybenzylamine. Thus, the electro donating on the amine does influence the reaction rate as expected. For amines with larger electro donating effects such as 2,4-dimethoxyaniline the reaction rate should be even larger since there is no CH_2 group in between the aromatic ring and the amine.

3.2.9. Repetition experiments

Two repetition experiments were compared for the ester amidation (experiments 11 and 17). The conversion versus time graph for these two experiments are illustrated in figure 27.

Figure 27: Repetition experiments of ester amidation at 83°C. Data points are connected for guidance of the eye

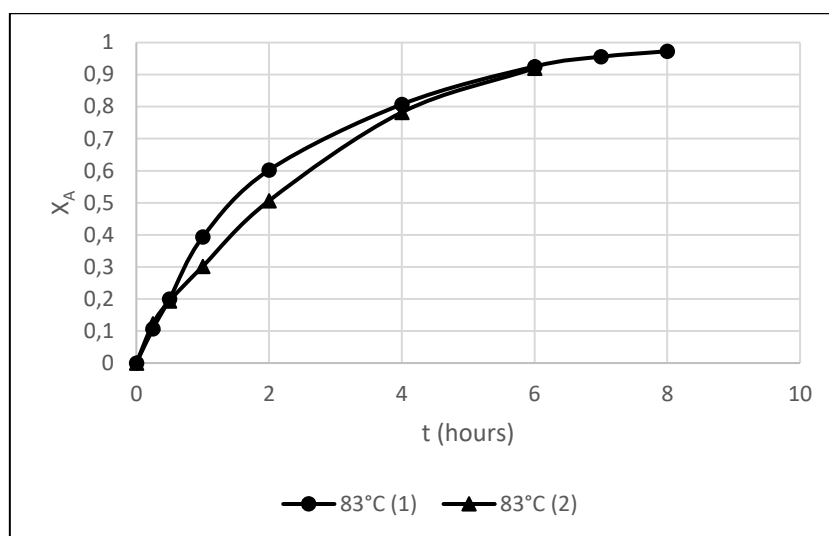Figure 27 shows that there is almost no difference between the two experiments. The average standard deviation between the conversions for the two experiments is equal to 0.0242. The ester amidation seems more repeatable than the *N*-carboxy benzylation. This could be because, for the *N*-carboxy benzylation, a variation of CO_2 concentration could be induced due to sampling for the ^{1}H-NMR analysis. The reason is because the cap together with the CO_2 filled balloon are removed for a few seconds during each measurement. For the ester amidation, small variations in volume could be induced during sampling. Here only the condenser is lifted slightly for a few seconds to take a sample. This could lower the volume slightly but it does not seem significant from the repetition experiments.

3.3. One-pot experiment

The reaction conditions used for the one-pot experiment are shown by table 15. The step 1 reaction was first conducted for 2 hours to form intermediate A, and then the step 2 reagent and catalyst are added in the same round bottom flask.

Table 15: Reaction conditions of one-pot experiment

Experiment	Catalyst after 2 hours	T (°C) start	T (°C) After 2 hours	C_{D0} (M)	C_{F0} (M)	C_{B0} (M) after 2 hours	Molar ratio (D:F)	Molar ratio after 2 hours (A:B)
19	Eco-Fe	30	83 (reflux)	0.242	0.233	0.233	1:1	1:1

This reaction was not successful in obtaining the target compound. After 2 hours, 91.0 % of intermediate was formed. But after adding the catalyst and amine, the intermediate did not react further to form the final product. Thus, performing the 2 reactions without purification steps in between was not successful in this study. Minor purifications could make the reaction possible such as a filtration to remove the Cs_2CO_3 solid phase. Further optimization for the one-pot reaction should be investigated in

another study because it has a potential of saving solvents which are used during purification with chromatography and also the overall time of the synthesis.

This work aimed to synthesize new potential anti-ageing compounds targeting RAGE. The synthetic strategy envisaged was a two-step procedure: *N*-carboxy benzylation of methyl L-pyroglutamate followed by an amidation reaction of the resulting methyl ester with 2,4-dichlorobenzylamine. Upon completion of the two-step synthesis, the optimization of each synthetic step was investigated in order to study the possibility of a one-step procedure for these chemical transformations.

The optimization for the *N*-carboxy benzylation was only successful for the temperature. For this first step reaction of the synthesis an optimum temperature was found at 30°C. The diffusion of CO_2 in the solution seemed to be the rate limiting step at a temperature around 30°C. Finding a greener solvent than ACN was not successful for this reaction. The other solvents, 2-MeTHF and dimethyl carbonate did not result in obtaining the target molecule. However, ACN itself is not the worst solvent because it has relatively low health hazards.

The optimization for the second step ester amidation reaction was more successful. However, the target molecule was not obtained with the methyl carboxy benzyl L-pyroglutamate nor with the bulky L-tertiary butyl carboxy benzyl pyroglutamate. The carboxy group on the lactam nitrogen atom seems responsible for the ring opening reaction during the ester amidation.

The use of ecocatalysts for this reaction resulted in a better reaction rate. The ecocatalyst rich in iron gave the best results for the reaction rate. This is an improvement on making this synthesis greener.

The concentration effect experiments showed that only the concentration of methyl *N*-carboxy benzyl pyroglutamate influenced the reaction rate. The overall order of the reaction was first order, with first order for methyl *N*-carboxy benzyl pyroglutamate and zeroth order for 2,4-dichlorobenzylamine. Thus, increasing the concentration of methyl *N*-carboxy benzyl pyroglutamate in the reaction mixture has a positive effect on the reaction rate.

The optimum temperature for the step 2 reaction is 83°C, which is the reflux temperature of ACN. The kinetic parameters for this reaction are also determined, which resulted in a model that can be used to simulate the reaction rate at other temperatures and concentrations. These are specifically when using the ecocatalyst rich in iron and ACN as solvent. The same method as in this thesis can be followed to determine the kinetic parameters for other catalysts and solvents.

The structure of the amine also showed to have an effect on the reaction rate. Using an amine such as 2,4-dimethoxybenzylamine with a larger electro donating effect than 2,4-dichlorobenzylamine resulted in a higher reaction rate, which is an improvement in time reduction of the reaction.

The one-pot experiment was not successful in this study. More investigation on this is required since this could reduce the use of solvents and the overall time spent on the synthesis. Further studies on the ring opening reaction are needed, such as an ester amidation with an amide group instead of the carboxyl group to see if this would also open the ring. There is also a need for more precise dosing of CO_2 to be able to determine the order of this reagent in the *N*-carboxy benzylation reaction. This would make it possible to determine the activation energy of this reaction. It could also be interesting to investigate other green solvents that could serve as a reaction medium for both reactions. As a validation on the electronic effect, other amines such as 2,4-dimethoxyaniline, 2,4-dichloroaniline, 2,4-dimethylaniline and 2,4-dimethylbenzylamine could be tested. This could give a more detailed view on the electronic effect of the amine. Further investigation on the interaction effect of the different parameters is needed such as for example between the temperature and catalysts or amines.
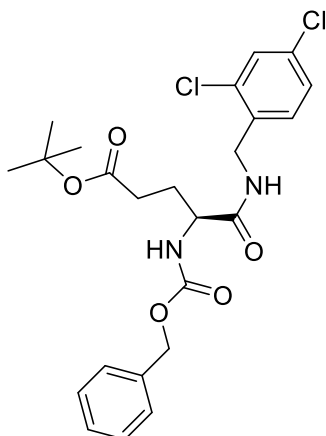
The physicochemical characterization of all new synthesized molecules, not mentioned in the literature, are described here.

4.1.   *Tert*-butyl (*S*)-4-(((benzyloxy)carbonyl)amino)-5-((2,4-dichlorobenzyl)amino)-5-oxopentanoate

Structure:

Protocol: This reaction was done in 5 mL ACN with 100 mg of Eco-Fe.

Table 16: Quantity of reagents for the reaction protocol of tertiary butyl analogue

Reagents	Molar mass (g/mol)	n (mmoles)	Mass (g)	Density (g/ml)	Volume (ml)
t-Butyl *N*-carboxy benzyl pyroglutamate	319.36	1.93	0.6155	/	/
2,4-dichlorobenzylamine	176.04	2.08	0.3662	1.308 (25°C)	0.28

Aspect: white solid

Molecular formula: $C_{24}H_{28}Cl_2N_2O_5$

Molecular weight: 494.39 g/mol

Yield: 12.3 %

R_f (EtOAc/*n*-heptane 60/40): 0.55

mp (acetonitrile): 130.0-131.4°C

IR υ cm^{-1}: 3283 (NH), 1736 (CO ester), 1688 (CO lactam), 1647 (CO carbamate), 746 (CCl), 697 (CCl)

^{1}H NMR (400 MHz, CDCl$_3$) δ (ppm): 1.45 (s, 9H, 3CH_3) 1.90-1.95 (m, 1H, CH$_2$CH_2CH), 2.20-2.29 (m, 3H, CH_2CH_2CH), 4.23 (s, 1H, CH), 4.47 (s, 2H, NHCH_2Ar), 5.00 (s, 2H, OCH_2Ar), 5.51 (d, J = 5.6 Hz, 1H, NH), 6.46 (s, 1H, NH), 7.20 (d, J = 8.4 Hz, 1H, ArH), 7.26-7.38 (m, 7H, ArH).

^{13}C NMR (100 MHz, CDCl$_3$) δ (ppm): 28.0 (3CH$_3$), 29.4 (CH$_2$), 32.5 (CH$_2$), 41.0 (CH$_2$), 53.9 (CH$_2$), 67.1 (CH), 127.3 (CH), 128.1 (CH), 128.1 (CH), 128.3 (CH), 128.3 (CH), 128.6 (CH), 128.6 (CH) 129.3 (CH), 131.0 (C), 133.9 (C), 134.2 (C), 134.4 (C), 136.2 (C), 156.4 (CO), 171.0 (CO), 172.0 (CO).

4.2. Methyl (*S*)-4-(((benzyloxy)carbonyl)amino)-5-((2,4-dichlorobenzyl)amino)-5-oxopentanoate
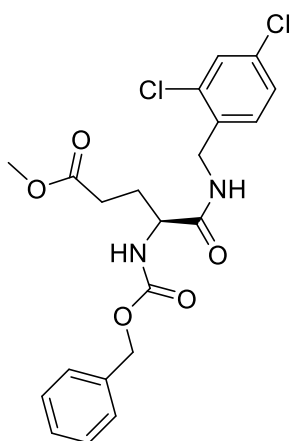
Structure:

Protocol: This reaction was done in 5 mL ACN with 100 mg of Eco-Fe.

Table 17: Quantity of reagents for the reaction protocol of opened ring structure

Reagents	Molar mass (g/mol)	n (mmoles)	Mass (g)	Density (g/ml)	Volume (ml)
Methyl *N*-carboxy benzyl pyroglutamate	277.28	2.13	0.5919	/	/
2,4-dichlorobenzylamine	176.04	1.80	0.3170	1.308 (25°C)	0.28

Aspect: white solid

Molecular formula: C$_{21}$H$_{21}$Cl$_2$N$_2$O$_5$

Molecular weight: 452.31 g/mol

Yield: 64.3%

R$_f$ (EtOAc/*n*-heptane 40/60): 0.34

mp (*n*-heptane): 134.1-136.1°C

**IR υ cm^{-1}:** 3317 (NH), 1737 (CO ester), 1689 (CO lactam), 1648 (CO carbamate), 760 (CCl), 697 (CCl).

^{1}H NMR (400 MHz, CDCl$_3$) δ (ppm): 1.95-2.00 (m, 1H, CH$_2$C*H*$_2$CH), 2.22-2.26 (m, 2H, C*H*$_2$CH$_2$CH), 2.28-2.32 (m, 1H, CH$_2$C*H*$_2$CH), 3.73 (s, 3H, CO$_2$C*H3*), 4.34-4.40 (m, 1H, C*H*), 4.46 (d, *J* = 5.6 Hz, 2H, NHC*H*$_2$Ar), 5.09 (s, 2H, OC*H*$_2$Ar), 5.59 (d, *J* = 8.0 Hz, 1H, N*H*), 6.30 (s, 1H, N*H*), 7.19 (dd, *J* = 6.4, 2.0 Hz, 1H, Ar*H*), 7.30-7.34 (m, 5H, Ar*H*), 7.37 (d, *J* = 2.0 Hz, 1H, Ar*H*).

^{13}C NMR (100 MHz, CDCl$_3$) δ (ppm): 28.7 (*C*H$_2$), 32.3 (*C*H$_2$), 41.0 (*C*H$_2$), 52.6 (*C*H$_2$), 53.4 (*C*H$_3$), 67.2 (*C*H), 127.4 (*C*H), 128.1 (*C*H), 128.1 (*C*H), 128.3 (*C*H), 128.6 (*C*H), 128.6 (*C*H), 128.6 (*C*H), 129.3 (*C*H), 131.1 (*C*), 133.9 (*C*), 134.2 (*C*), 136.1 (*C*), 156.3 (*C*O), 171.8 (*C*O), 172.3 (*C*O).

LC/MS (APCI$^+$) *m/z*: 453.0 (MH$^+$) (calcd for C$_{21}$H$_{21}$Cl$_2$N$_2$O$_5$: 452.31 g/mol), tr 19.1 min.

4.3. Methyl (*S*)-4-(((benzyloxy)carbonyl)amino)-5-((2,4-dimethoxybenzyl)amino-5-oxopentanoate

Structure :
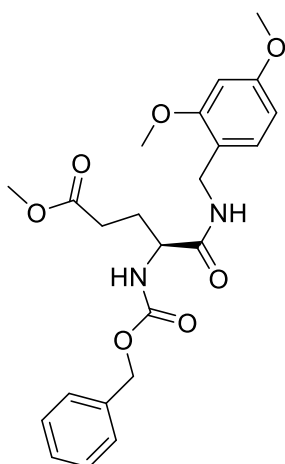
Protocol: This reaction was done in 5 mL ACN with 0.05 equivalent of ZrCl$_4$.

Table 18: Quantity of reagents for the reaction protocol of methoxy analogue

Reagents	Molar mass (g/mol)	n (mmoles)	Mass (g)	Density (g/ml)	Volume (ml)
Methyl *N*-carboxy benzyl pyroglutamate	277.28	1.82	0.5041	/	/
2,4-dimethoxybenzylamine	167.04	1.80	0.3070	1.113 (25°C)	0.27

Aspect: white solid

Molecular formula: C$_{23}$H$_{28}$Cl$_2$N$_2$O$_7$

Molecular weight: 443.48 g/mol

Yield: 19.3%

R$_f$ (EtOAc/*n*-heptane 40/60): 0.21

mp (*n*-heptane): 115.9-120°C

IR υ cm^{-1}: 3306 (NH), 1744 (CO ester), 1684 (CO lactam), 1211 (CO), 693 (CCl)

^{1}H NMR (400 MHz, CDCl$_3$) δ (ppm): 1.98-2.00 (m, 1H, CH$_2$C*H$_2$*CH), 2.17-2.27 (m, 3H, C*H$_2$*CH$_2$CH), 3.72 (s, 3H, CO$_2$C*H$_3$*), 3.79 (s, 3H, OC*H$_3$*), 3.82 (s, 3H, OC*H$_3$*), 4.33 (d, *J* = 6.0 Hz, 3H, C*H*CONHC*H$_2$*), 5.09 (s, 2H, OC*H$_2$*Ar), 5.69 (d, *J* =8.0 Hz, 1H, N*H*), 6.05 (s, 1H, N*H*), 6.40-6.45 (m, 2H, Ar*H*), 7.16 (d, *J* = 8.4 Hz, 1H, Ar*H*), 7.26-7.34 (m, 5H, Ar*H*).

^{13}C NMR (100 MHz, CDCl$_3$) δ (ppm): 28.3 (*C*H$_2$), 32.5 (*C*H$_2$), 39.1 (*C*H$_2$), 52.5 (*C*H$_2$), 53.6 (*C*H$_3$), 55.4 (*C*H$_3$), 55.4 (*C*H$_3$), 67.0 (*C*H), 98.6 (*C*H), 103.9 (*C*H), 118.7 (*C*H), 128.1 (*C*H), 128.2 (*C*H), 128.4 (*C*H), 128.4 (*C*H), 128.5 (*C*H), 130.6 (*C*), 136.3 (*C*), 156.2 (*C*), 158.6 (*C*), 160.6 (*C*O), 171.2 (*C*O), 172.5 (*C*O).

BIBLIOGRAPHY

[1]   E. MacArthur, "Ellenmacarthurfoundation.org." https://ellenmacarthurfoundation.org/circulate-products-and-materials (accessed Apr. 08, 2022).

[2]   F. Roschangar, R. A. Sheldon, and C. H. Senanayake, "Overcoming barriers to green chemistry in the pharmaceutical industry – the Green Aspiration Level TM concept †," pp. 752–768, 2015, doi: 10.1039/c4gc01563k.

[3]   M. Meinshausen *et al.*, "Greenhouse-gas emission targets for limiting global warming to 2 °C," *Nature*, vol. 458, no. 7242, pp. 1158–1162, 2009, doi: 10.1038/nature08017.

[4]   G. Homerin, A. S. Nica, A. Aitouche, B. Rigo, E. Lipka, and A. Ghinet, "Carbon dioxide transformation as a green alternative to phosgene and chloroformates: *N*-carboxyalkylation of lactams and analogues," *J. CO$_2$ Util.*, vol. 54, no. September, p. 101782, 2021, doi: 10.1016/j.jcou.2021.101782.

[5]   C. Hepburn *et al.*, "The technological and economic prospects for CO_2 utilization and removal," *Nature*, vol. 575, no. September 2018, pp. 87–97, 2019, doi: 10.1038/s41586-019-1681-6.

[6]   JUNIA HEI, "LABORATOIRE DE CHIMIE DURABLE ET SANTÉ." https://www.junia.com/innovation-recherche/plateformes-dinnovation-et-de-recherche/laboratoire-de-chimie-durable-et-sante/#:~:text=Le laboratoire de Chimie Durable,stimulateurs de défense des plantes. (accessed May 01, 2022).

[7]   Z. Wang, *Comprehensive Energy Systems*. Hangzhou, 2018.

[8]   A. Aitouche, "nweurope.eu," *Interreg North-West Europe River*. https://www.nweurope.eu/projects/project-search/river-non-carbon-river-boat-powered-by-combustion-engines/ (accessed Mar. 11, 2022).

[9]   S. Bongarzone, V. Savickas, F. Luzi, and A. D. Gee, "Targeting the Receptor for Advanced Glycation Endproducts (RAGE): A Medicinal Chemistry Perspective," *J. Med. Chem.*, vol. 60, no. 17, pp. 7213–7232, 2017, doi: 10.1021/acs.jmedchem.7b00058.

[10]   P. K. Sahoo, Y. Zhang, and S. Das, "CO2-promoted reactions: An emerging concept for the synthesis of fine chemicals and pharmaceuticals," *ACS Catal.*, vol. 11, no. 6, pp. 3414–3442, 2021, doi: 10.1021/acscatal.0c05681.

[11]   M. Bhat, S. L. Belagali, S. V. Mamatha, B. K. Sagar, and E. V. Sekhar, *Importance of quinazoline and quinazolinone derivatives in medicinal chemistry*, vol. 71. 2021.

[12]   G. Homerin *et al.*, "ZrCl$_4$ as a new catalyst for ester amidation: An efficient synthesis of h-P2X7R antagonists," *Tetrahedron Lett.*, vol. 57, no. 10, pp. 1165–1170, 2016, doi: 10.1016/j.tetlet.2016.02.004.

[13]   K. Deleersnyder, *Lanthanide-mediated organic synthesis: lanthanide (III) compounds as Lewis acid catalysts and cerium (IV) compounds as reagents for reactions in ionic*. 2007.

[14]   T. Guérin *et al.*, "Ecocatalysed Hurtley reaction: Synthesis of urolithin derivatives as new potential RAGE antagonists with anti-ageing properties," *Sustain. Chem. Pharm.*, vol. 23, no. September, 2021, doi: 10.1016/j.scp.2021.100518.

[15]   M. Cvjetko Bubalo, S. Vidović, I. Radojčić Redovniković, and S. Jokić, "Green solvents for green technologies," *J. Chem. Technol. Biotechnol.*, vol. 90, no. 9, pp. 1631–1639, 2015, doi: 10.1002/jctb.4668.

[16]   S. Mallakpour and Z. Rafiee, *Green Solvents Fundamental and Industrial Applications BT - Green Solvents I: Properties and Applications in Chemistry*. 2012.

[17]   C. Capello, U. Fischer, and K. Hungerbühler, "What is a green solvent? A comprehensive framework for the environmental assessment of solvents," *Green Chem.*, vol. 9, no. 9, pp. 927–93, 2007, doi: 10.1039/b617536h.

[18]   M. Décultot, A. Ledoux, M. C. Fournier-Salaün, and L. Estel, "Solubility of CO2 in methanol, ethanol, 1,2-propanediol and glycerol from 283.15 K to 373.15 K and up to 6.0 MPa," *J. Chem. Thermodyn.*, vol. 138, pp. 67–77, 2019, doi: 10.1016/j.jct.2019.05.003.

[19]   O. Levenspiel *et al.*, *Chemical reaction engineering*, vol. 35, no. 9. 1980.

[20]   E. Van Hoof and L. Thomassen, "ereiding en toepassingen van aromatische carbonylverbindingen," in *Methodiek van de organische synthese*, Diepenbeek, 2021, pp. 20–26.

[21]   G. Cudiamat, "Flash Chromatography," *LCGC North Am.*, vol. 38, no. 3, 2020.

[22]   B. Bickler, "What is Flash Chromatography and why should I do it?," *Biotage*, 2019. https://selekt.biotage.com/blog/what-is-flash-chromatography-and-why-do-i-need-to-do-it (accessed Apr. 03, 2022).

[23]   H. Kramer and G. Van Rosmalen, "CRYSTALLIZATION," in *Encyclopedia of Seperation Science*, Delft: Academic press, 2003, pp. 64–84.

[24]   A. Sandtorv, "TLC-Analysis," 2021. https://chem.libretexts.org/Bookshelves/Organic_Chemistry/Organic_Chemistry_Lab_Techniq ues_(Nichols)/02%3A_Chromatography/2.03%3A_Thin_Layer_Chromatography_(TLC)#:~:te xt=Thin layer chromatography (TLC) is,uses a different stationary phase.&text=TLC is a c (accessed Apr. 04, 2022).

[25]   Sigmaaldrich, "Nuclear magnetic resonance." https://www.sigmaaldrich.com/BE/en/applications/analytical-chemistry/nuclear-magnetic-resonance (accessed Apr. 03, 2022).

[26]   J. Ashenhurst, "Stereochemistry and Chirality," 2021. https://www.masterorganicchemistry.com/2017/02/07/optical-rotation-optical-activity-and-specific-rotation/#five (accessed May 20, 2022).

[27]   D. Kennepohl, S. Farmer, T. Soderberg, Z. Sharrett, and K. Cunningham, "Polarimetry," 2019. https://chem.libretexts.org/Courses/Purdue/Purdue%3A_Chem_26505%3A_Organic_Chemistr y_I_(Lipton)/Chapter_5._Spectroscopy/5.5_Polarimetry (accessed May 20, 2022).

[28]   P. M. V. Raja and A. R. Barron, "Melting Point Analysis," 2021. https://chem.libretexts.org/Bookshelves/Analytical_Chemistry/Physical_Methods_in_Chemistr y_and_Nano_Science_(Barron)/02%3A_Physical_and_Thermal_Analysis/2.01%3A_Melting_ Point_Analysis#:~:text=Melting point analysis%2C as the,used to identify the sample. (accessed Jun. 01, 2022).

[29]   S. Ross, "Basic principles of chemical kinetics," in *in kinetics of enzyme action: Essential principles for drug hunters*, John Wiley & Sons, 2011, p. 261.

[30]   P. Dufrénoy *et al.*, "Valorisation en synthèse organique d ' éco -catalyseurs hétérogènes régénérables à partir de matériaux verts cultivés sur des sols contaminés Présentée et soutenue par," Normandie Université, 2018.